

# Dark-Matter Neutrino interactions in the early universe

M.Sc. Thesis

by

Sahil Rawat



DISCIPLINE OF PHYSICS  
INDIAN INSTITUTE OF TECHNOLOGY  
INDORE, INDIA

MAY, 2024

# Dark-Matter Neutrino interactions in the early universe

M.Sc. Thesis

*Submitted in partial fulfilment of the  
requirements for the award of the degree*

*of*

Master of Science

by

Sahil Rawat



DISCIPLINE OF PHYSICS  
INDIAN INSTITUTE OF TECHNOLOGY  
INDORE, INDIA

MAY, 2024

# Candidate's Declaration

I hereby certify that the work which is being presented in the thesis entitled **Dark-Matter Neutrino interactions in the early universe** in the partial fulfillment of the requirements for the award of the degree of **MASTER OF SCIENCE** and submitted in the **DISCIPLINE OF PHYSICS, Indian Institute of Technology Indore**, is an authentic record of my own work carried out during the time period from July, 2022 to May 2024 under the supervision of **Prof. Subhendu Rakshit, Indian Institute of Technology Indore**.

The matter presented in this thesis has not been submitted by me for the award of any other degree of this or any other institute.

Sahil  
13/05/24

Signature of the student with date

---

This is to certify that the above statement made by the candidate is correct to the best of my/our knowledge.

Subhendu Rakshit

Signature of Thesis Supervisor

---

**Mr. Sahil Rawat** has successfully given his M.Sc. Oral Examination held on 15 May, 2024.

Subhendu Rakshit  
Signature of Thesis Supervisor

Date: 15-05-2024

Mahendra Nath

Convener, DPGC

Date: 24/05/2024

# Acknowledgments

I would like to express my deepest gratitude to my supervisor, Prof. Subhendu Rakshit. His exceptional guidance, unwavering support, and tireless dedication have been invaluable. I am immensely grateful for his efforts throughout this project and beyond, spanning multiple dimensions.

I am also deeply grateful to Dhruv bhaiya in my lab for his invaluable mentorship and assistance and for sharing his wisdom of life.

I would like to extend a lighthearted acknowledgment to my friends who provided much-needed distraction when deadlines loomed large (sarcastic laughs). You people were a reminder that work-life balance is key (even if we sometimes leaned more towards the “life” side). Cheers to friendship and inside jokes that kept us going!

# Abstract

The presence and characteristics of Dark Matter (DM) are inferred indirectly through observed gravitational effects in astronomy and cosmology. These effects include the direct observation of weak gravitational lensing near clusters, the study of missing mass in clusters and galaxies, the structure of galactic rotation curves, and the correlation between cosmic microwave background anisotropies and the large-scale structure of the universe. These phenomena collectively suggest the existence of DM as a plausible explanation.

The Standard Model of particle physics (SMPP) is currently the leading theory for describing all known fundamental particles, except gravity. While the SMPP successfully incorporates three of the four fundamental forces, it lacks a suitable candidate for Dark Matter.

Therefore, the shortcomings of the SMPP necessitate the development of new physics models capable of addressing these limitations. Such models may have significant implications for understanding the early history of the universe.

This thesis focuses on exploring interactions between neutrinos and DM. If neutrinos interacted with dark matter in the early universe, it could have affected the evolution and distribution of neutrinos over cosmic time. Such interactions might have led to changes in the neutrino abundance that persist to this day. Consequently, if the number density of neutrinos is different from what is predicted solely by standard cosmological models, this could affect the expected rate of neutrino capture events in detectors like PTOLEMY.

# Contents

<b>Candidate Declaration</b>	<b>ii</b>
<b>Acknowledgements</b>	<b>iii</b>
<b>Abstract</b>	<b>iv</b>
List of Figures . . . . .	vii
<b>1 Prelude</b>	<b>1</b>
<b>2 Introduction</b>	<b>3</b>
2.1 Motivation . . . . .	5
<b>3 The Standard Model of cosmology</b>	<b>7</b>
3.1 Expansion of Universe . . . . .	7
3.2 Einstein equations . . . . .	9
3.3 Robertson-Walker metric . . . . .	9
3.4 Ricci tensor and Ricci scalar . . . . .	10
3.5 Energy-momentum tensor . . . . .	12
3.6 Friedmann Equations . . . . .	12
3.7 Number density, Energy density, and Pressure . . . . .	14
3.8 Entropy . . . . .	18
3.9 Neutrino decoupling . . . . .	22
3.10 Big Bang Nucleosynthesis . . . . .	24
3.10.1 Neutrons and Protons . . . . .	24
3.10.2 Deuterium . . . . .	26

3.10.3 Helium and Heavier Nuclei . . . . .	29
3.11 Recombination . . . . .	30
3.12 Baryon acoustic oscillations . . . . .	35
<b>4 Detection prospects of CNB at PTOLEMY</b>	<b>37</b>
4.1 Neutrino capture by neutron . . . . .	38
4.2 Neutrino absorption by tritium . . . . .	40
4.3 Results . . . . .	43
<b>5 Dark matter particle</b>	<b>44</b>
5.1 WIMP Dark Matter . . . . .	44
5.1.1 Boltzmann Equation . . . . .	45
5.1.2 Numerical Integration . . . . .	47
5.2 DM- $\nu$ decoupling . . . . .	48
5.3 Effective number of neutrinos: $N_{\text{eff}}$ . . . . .	49
5.4 Evidence of DM- $\nu$ interaction on PTOLEMY . . . . .	51
<b>6 Results and Discussion</b>	<b>54</b>
<b>A Cross section for neutrino capture on tritium</b>	<b>56</b>

# List of Figures

1.1	Cosmic Microwave Background (CMB) . . . . .	2
3.1	The universe is expanding, causing the physical distance between stationary co-moving coordinates to grow over time.	8
3.2	The presence of light nuclei in the early universe . . . . .	29
3.3	Baryonic acoustic oscillations observed in the galaxy distribution. [7] . . . . .	36
5.1	A numerical solution to the Boltzmann equation is applied for parameters where $m = 100\text{GeV}$ , $g_* = 100$ , and $\langle\sigma_{ann}v\rangle = 10^{-9}\text{GeV}^{-2}$ . Overlaid on this solution is the equilibrium value $y_{\text{eq}}$ . . . . .	48
5.2	The decoupling of neutrino from DM . . . . .	49

# Chapter 1

## Prelude

Every civilization crafts an origin narrative, and we believe we have crafted the most accurate one yet.

Our narrative, known as the Big Bang theory, carries a captivating name that can initially mislead. Contrary to common perception, the theory does not propose that the universe began with a literal “bang”. In truth, the Big Bang theory does not address the inception of the universe at all. The straightforward response to the question “how did the universe begin?” remains “we don’t know.”

Instead, our narrative modestly describes the early universe’s characteristics. It begins with a fundamental observation: the universe is expanding. This expansion implies that in earlier epochs, all matter was in closer proximity, resulting in higher temperatures. The Big Bang theory suggests that in the past, the universe was extraordinarily hot—so much so that matter, atoms, and nuclei were liquefied, filling space with a searing fireball. The Big Bang theory comprises a set of concepts, computations, and forecasts that elucidate events within this fireball and its subsequent evolution into the universe we observe today.

The term “theory” within the Big Bang theory may imply uncertainty, which is misleading. This theory is akin to the theory of evolution—it is a factual occurrence. We have observed the remnants of the fiery early

universe in the form of cosmic microwave background radiation, captured in a photograph (see Figure. 1.1), which contains abundant insights into the universe’s earlier state.

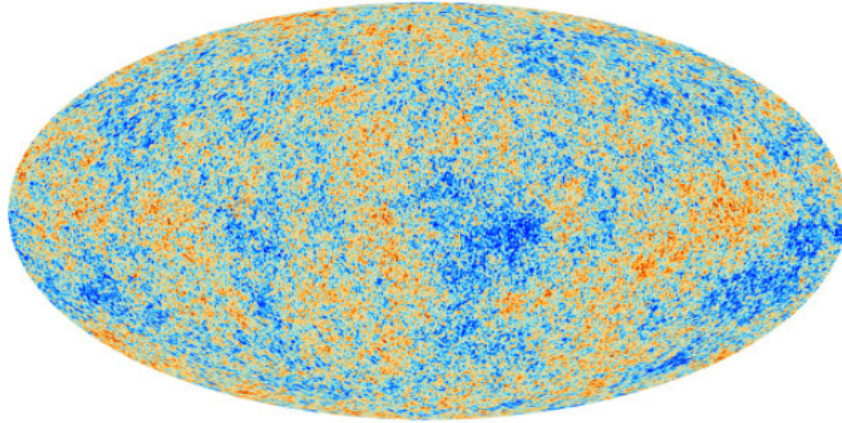


Figure 1.1: Cosmic Microwave Background (CMB)

As we approach the “ $t = 0$ ” moment colloquially referred to as “the Big Bang,” the universe becomes hotter, with energies escalating. Cosmology endeavors to trace back as close as feasible to this enigmatic moment. Remarkable strides have been made in this pursuit.

Our understanding extends to approximately a minute post-Big Bang, with meticulous calculations aligning perfectly with observations of elemental formation in the early universe. Further back in time, observational data becomes scarcer, but our grasp of particle physics instills confidence up to  $t = 10^{-12}$  seconds post-Big Bang. Moreover, there are compelling indications of a rapid cosmic expansion phase termed inflation occurring even earlier.

Discussing the universe’s infancy, particularly moments mere minutes or fractions of seconds old, might seem surreal. Nevertheless, numerous surviving clues from those eras can be elucidated with remarkable precision by applying basic, well-established physical principles to these extreme conditions.

# Chapter 2

## Introduction

The  $\Lambda$ CDM model, the standard framework of cosmology, has been firmly established through cosmological observations, particularly the precise mapping of Cosmic Microwave Background (CMB) anisotropies. This model provides a straightforward yet effective explanation for several key aspects:

- The presence and characteristics of the cosmic microwave background
- The large-scale distribution of galaxies across the universe
- The observed ratios of hydrogen, helium, and lithium in the universe
- The observed accelerated expansion of the universe, as evidenced by distant galaxy and supernova light.

Furthermore, the  $\Lambda$ CDM predicts the existence of a cosmic neutrino background (CNB) analogous to the cosmic microwave background (CMB). According to  $\Lambda$ CDM model, neutrinos decoupled from other standard model particles at an earlier epoch (around  $\sim 1$  second after the Big Bang) compared to CMB photons (around  $\sim 4 \times 10^5$  years) and formed the CNB. Detecting these neutrinos can provide crucial insights into the universe's earliest moments following the Big Bang.

The energy density contribution of CNB neutrinos influences the abundance of light elements during nucleosynthesis and leaves discernible imprints on CMB anisotropies and structure formation. These effects serve

as indirect indicators of the CNB’s presence. However, directly measuring CNB neutrinos poses substantial challenges due to their minuscule masses, weak interaction cross-sections, and low temperatures (approximately  $\sim 1.95$  Kelvin).

From Cosmological observation, we find that in our universe 85% of all matter is dark matter (DM). Dark matter is the composition of two words dark and matter, it is named “dark” because it does not interact with electromagnetic radiation (EMR) by reflecting, absorbing, or emitting it, so astronomers are still unable to observe it and therefore can only study its consequences on visible stuff and “matter” as it behaves like matter. Swiss astrophysicist Fritz Zwicky in 1933, studied the motion of the galaxies in the Coma cluster, during his research work at the California Institute of Technology, and summarized that DM exists. Following that, measurements of whirling spiral galaxies, the implications of gravitational lensing on background objects demonstrated the presence of DM, and numerous pieces of evidence such as the Bullet cluster and the PLANCK satellite were recorded. Furthermore, DM is an imperative ingredient in modelling and simulation of the early universe, the evolution of structures and galaxies, as well as having a detectable impact on CMB anisotropies.

The evolution of our universe is well described by the Standard Model of Cosmology (SMC), often known as the Hot Big Bang Model. The SMC, also known as the  $\Lambda$ CDM, is based on two key theoretical frameworks: the Standard Model of particle physics (SMPP), which covers physics at the quantum level, and the General Theory of Relativity (GTR), which covers physics at the classical level. It is based on the following assumptions:

- The universe evolved from pure energy in the Big Bang,
- The universe is made up of about 5% ordinary matter, 27% dark matter, and 68% percent dark energy,
- The universe is isotropic and homogeneous on a cosmological scale,

and

- DM is assumed to be cold dark matter(CDM).

However, there are issues when comparing SMC to SMPP, one of which is that no feasible candidate in particle physics (PP) satisfies all of the DM requirements. As a result, cosmology suggests that beyond the SMPP, new physics is required. This thesis aims to enlighten one part of the DM problem: DM interaction beyond gravity, i.e., DM- $\nu$  interaction. We wish to understand if such interactions are conceivable, what their impact would be, and how we may improve the accuracy of such models by applying cosmological constraints. Before going into a detailed study of the DM- $\nu$  interaction, we go through the Big Bang's underlying principles in section and its three major epochs that provide a piece of evidence for the presence of dark matter and predict its nature: Big Bang Nucleosynthesis (BBN), Cosmic Microwave Background (CMB), and Structure Formation. And we address various other pieces of evidence like the galactic rotational curve, and gravitational lensing that predicts the existence of dark matter. Then we mention briefly all of the suggested alternatives for DM candidate. We look for current DM status from collider search, direct search, and indirect search.

## 2.1 Motivation

For the past four decades, Collisionless Dark Matter (DM) has stood as the predominant paradigm. However, at a minimum, DM must have had interactions to be produced in the early Universe. Among these interactions, those involving neutrinos are particularly intriguing, given that neutrinos are among the few particles offering evidence of physics beyond the Standard Model (SM) to date. Naturally, this prompts the question of whether DM and neutrino properties are interconnected and whether direct interactions between these two species are possible.

The existence of non-vanishing DM-neutrino (DM- $\nu$ ) interactions carries significant cosmological and astrophysical implications. [12]

- These interactions can potentially account for the observed DM relic density if DM was thermally produced and annihilations into neutrinos represent the dominant channel.
- They may also generate signatures of DM in indirect detection scenarios, either through DM annihilating or decaying into neutrinos within the galaxy or via cosmic neutrino signals.
- Furthermore, DM- $\nu$  interactions might erase primordial DM fluctuations, thereby suppressing large-scale structures (LSS) in the Universe and reducing the number of satellites around Milky Way-like galaxies, potentially addressing the “too-big-to-fail” problem associated with cold DM.
- DM- $\nu$  interactions could play a role in generating neutrino masses within radiative models.
- Novel neutrino interactions can impede their free streaming even after the freeze-out of weak interactions. This leads to a phase shift in the acoustic peaks of the cosmic microwave background (CMB), potentially mitigating the Hubble tension.

These diverse implications underscore the importance of exploring DM- $\nu$  interactions and their potential ramifications for understanding the nature and behavior of both Dark Matter and neutrinos in the cosmic landscape.

# Chapter 3

## The Standard Model of cosmology

### 3.1 Expansion of Universe

According to Edwin Hubble in 1929, all galaxies are moving away from our galaxy at a rate which is proportional to their separation. The Doppler shift of spectral lines may be used to calculate the speed. The Big Bang model came into the picture as a result of this.

Let's look at how the universe has evolved with time, from the Big Bang to the present.

The universe will either grow or contract if it is thought to be isotropic and homogeneous. We consider two galaxies at  $r(t)$  and  $R(t)$  distances from our own. For isotropic and homogeneous expansion, the ratio

$$\chi = \frac{r(t)}{R(t)} \tag{3.1.1}$$

is constant in time. As a result, when we differentiate in terms of time, we obtain

$$H = \frac{\dot{R}}{R} \tag{3.1.2}$$

where,  $H$  is called the Hubble parameter that measures how rapidly the cosmos expands at various distances from a given location in space and  $R$  is the scale factor that has value 1 for the present universe. The wavelength of light ( $\lambda_s$ ) emitted by the source galaxy has been stretched out due to the expansion of the cosmos. So in terms of scale factor, the magnitude of the redshift ( $z$ ) is expressed as,

$$1 + z = \frac{\lambda_0}{\lambda_s} = \frac{1}{R(t)} \quad (3.1.3)$$

The wavelength of light that we detect is  $\lambda_0$ . If the recession speed ( $v$ ) of the galaxy is substantially slower than the speed of light then,  $z \approx v/c$ . Because a photon's energy is inversely related to its wavelength, we may express temperature in terms of scale factor as

$$T(t) = \frac{T_0}{R(t)} \quad (3.1.4)$$

where  $T_0$  is today's temperature of photons.

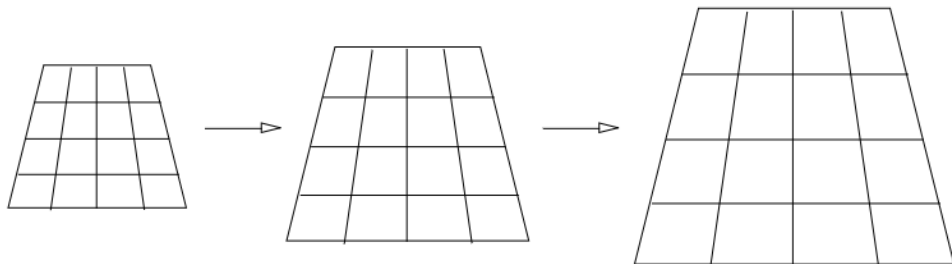


Figure 3.1: The universe is expanding, causing the physical distance between stationary co-moving coordinates to grow over time.

## 3.2 Einstein equations

Einstein equations are

$$R_{\mu\nu} - \frac{1}{2}g_{\mu\nu}R - \Lambda g_{\mu\nu} = 8\pi GT_{\mu\nu} \quad (3.2.1)$$

On the left-hand side, we have the Einstein tensor ( $G_{\mu\nu}$ ) with an additional term incorporating the cosmological constant, which becomes particularly significant in cosmological contexts.

On the right-hand side,  $G$  represents the universal gravitational constant, and  $T_{\mu\nu}$  denotes the energy-momentum tensor, defined explicitly as

$$T_{\mu\nu} = (\rho + p)u_\mu u_\nu - pg_{\mu\nu} \quad (3.2.2)$$

The metric  $g_{\mu\nu}$  characterizes the geometry of the manifold to which the equations pertain, and  $u_\alpha$  represents the macroscopic velocity of the medium within this context.

## 3.3 Robertson-Walker metric

Consider the Einstein tensor ( $G_{\mu\nu}$ ), which comprises a Ricci tensor and a Ricci scalar. To compute these tensors, we require a metric that specifically suits our final expressions for the homogeneous and isotropic universe. Therefore, we need to identify a metric ( $g_{\mu\nu}$ ) that encompasses all facets of the cosmological principle. The solution to this requirement is provided by the Robertson-Walker metric.

$$ds^2 = dt^2 - a^2(t) \left( \frac{1}{1 - \frac{r^2}{K^2}} dr^2 + r^2 d\theta^2 + r^2 \sin^2 \theta d\varphi^2 \right) \quad (3.3.1)$$

The Robertson-Walker metric characterizes an isotropic universe by lacking crossed terms between time and space, thus avoiding any privileged direction. Additionally, it describes a homogeneous universe due to its

spherical symmetry.

The quantity  $a(t)$ , known as the scale factor, represents the temporal variation in the relative distance between two points in the universe. The scale factor is set to 1 at the present time. Henceforth, the time dependence of the scale factor can be understood implicitly, simplifying to  $a(t) \equiv a$ .

### 3.4 Ricci tensor and Ricci scalar

To specialize Einstein's equations for a homogeneous and isotropic universe, we require the Ricci tensor and the Ricci scalar.

The first step is to compute the Christoffel symbols of the Robertson-Walker metric using the following formula:

$$\Gamma_{ji}^l = \frac{1}{2} g^{lm} (\partial_j g_{mi} + \partial_i g_{mj} - \partial_m g_{ij}) \quad (3.4.1)$$

The Robertson-Walker metric is beneficial for this calculation because it is diagonal and possesses a symmetric connection. Consequently, most of the Christoffel symbols will either be symmetric or zero. The non-zero Christoffel symbols are given by:

- $\Gamma_{rr}^t = \frac{a\dot{a}}{1-\frac{r^2}{K^2}}$
- $\Gamma_{\theta\theta}^t = r^2 a\dot{a}$
- $\Gamma_{\varphi\varphi}^t = r^2 a\dot{a} \sin^2 \theta$
- $\Gamma_{tr}^r = \Gamma_{rt}^r = \Gamma_{t\theta}^\theta = \Gamma_{\theta t}^\theta = \Gamma_{t\varphi}^\varphi = \Gamma_{\varphi t}^\varphi = \frac{\dot{a}}{a}$
- $\Gamma_{rr}^r = \frac{r}{K^2(1-\frac{r^2}{K^2})}$
- $\Gamma_{\theta\theta}^r = -r \left(1 - \frac{r^2}{K^2}\right)$
- $\Gamma_{\varphi\varphi}^r = -r \left(1 - \frac{r^2}{K^2}\right) \sin^2 \theta$
- $\Gamma_{r\theta}^\theta = \Gamma_{\theta r}^\theta = \Gamma_{r\varphi}^\varphi = \Gamma_{\varphi r}^\varphi = \frac{1}{r}$

- $\Gamma_{\varphi\varphi}^{\theta} = -\sin\theta \cos\theta$
- $\Gamma_{\varphi\theta}^{\varphi} = \Gamma_{\theta\varphi}^{\varphi} = \frac{1}{\tan\theta}$

Once the Christoffel symbols have been computed, we can proceed to calculate the Riemann tensor

$$R_{kji}^l = \partial_i \Gamma_{kj}^l - \partial_j \Gamma_{ki}^l + \Gamma_{kj}^m \Gamma_{mi}^l - \Gamma_{ki}^m \Gamma_{mj}^l \quad (3.4.2)$$

In fact, our focus lies solely on the components of the Riemann tensor where the top index matches the middle bottom index. These specific components are essential for computing the Ricci tensor ( $R_{imj}^m$ ). The non-zero components of the Ricci tensor are

- $R_{tt} = R_{tmt}^m = R_{trt}^r + R_{t\theta t}^{\theta} + R_{t\varphi t}^{\varphi} = -3\frac{\ddot{a}}{a}$
- $R_{rr} = R_{rmr}^m = \frac{a\ddot{a}}{1-\frac{r^2}{K^2}} + \frac{2\dot{a}^2}{1-\frac{r^2}{K^2}} + \frac{2}{K^2(1-\frac{r^2}{K^2})}$
- $R_{\theta\theta} = R_{\theta m\theta}^m = r^2 a\ddot{a} + 2r^2 \dot{a}^2 + 2\frac{r^2}{K^2}$
- $R_{\varphi\varphi} = R_{\varphi m\varphi}^m = r^2 a\ddot{a} \sin^2\theta + 2r^2 \dot{a}^2 \sin^2\theta + 2\frac{r^2}{K^2} \sin^2\theta$

Observing the diagonal nature of the Ricci tensor, we can summarize the findings by stating

$$R_{tt} = -3\frac{\ddot{a}}{a} \quad (3.4.3)$$

$$R_{ii} = \frac{-g_{ii}}{a^2} (a\ddot{a} + 2\dot{a}^2 + 2K^{-2}) \quad (3.4.4)$$

Ultimately, we obtain the Ricci scalar:

$$R = g^{ik} R_{ik} = -6\frac{\ddot{a}}{a} - 6\left(\frac{\dot{a}}{a}\right)^2 - 6\frac{1}{K^2 a^2} \quad (3.4.5)$$

## 3.5 Energy-momentum tensor

By definition, a perfect fluid is isotropic, meaning it appears uniform regardless of the direction of observation. Therefore, the macroscopic velocity of the fluid lacks a preferred direction and consists solely of a temporal component:  $u^\alpha = (1, 0, 0, 0)$ .

It's important to note that  $u^t = 1$  due to the constraints of special relativity.

$$(u^\alpha)^2 = g_{\alpha\beta}u^\alpha u^\beta = c^2 = 1 \Rightarrow g_{tt} (u^t)^2 = c^2 \Leftrightarrow u^t = 1 \quad (3.5.1)$$

The energy-momentum tensor for a perfect fluid exhibits a diagonal form, and its components are

$$T_{tt} = \rho g_{tt} \quad (3.5.2)$$

$$T_{ii} = -p g_{ii} \quad (3.5.3)$$

In our derivation, we consider the universe as being filled with a perfect fluid, which adheres to the cosmological principle.

## 3.6 Friedmann Equations

In preceding sections, we have computed and derived all necessary elements to achieve our objective. Now, we are prepared to incorporate these elements into Einstein's equations.

The equations that will deviate from zero are specifically those with matching indices, given the diagonal nature of our metric.

Thus, we commence with the temporal component:

$$R_{tt} - \frac{1}{2}Rg_{tt} - \Lambda g_{tt} = 8\pi G\rho u_t u_t \quad (3.6.1)$$

$$-3\frac{\ddot{a}}{a} + 3\frac{\ddot{a}}{a} + 3\left(\frac{\dot{a}}{a}\right)^2 + 3\frac{1}{K^2a^2} - \Lambda = 8\pi G\rho(t) \quad (3.6.2)$$

We arrive at

$$\left(\frac{\dot{a}(t)}{a(t)}\right)^2 = \frac{8\pi G}{3}\rho(t) + \frac{\Lambda}{3} - \frac{1}{K^2a^2(t)} \quad (3.6.3)$$

Now we can examine the spatial part. For each spatial component, we arrive at the identical equation

$$\frac{-g_{ii}}{a^2(t)} \left( a\ddot{a} + 2\dot{a}^2 + \frac{2}{K^2} \right) - \frac{1}{2}Rg_{ii} - \Lambda g_{ii} = 8\pi G(-p)g_{ii} \quad (3.6.4)$$

By eliminating the metric from both sides, we derive

$$-\frac{\ddot{a}}{a} - 2\left(\frac{\dot{a}}{a}\right)^2 - \frac{2}{K^2a^2} + 3\frac{\ddot{a}}{a} + 3\left(\frac{\dot{a}}{a}\right)^2 + \frac{3}{K^2a^2} - \Lambda = -8\pi Gp \quad (3.6.5)$$

$$\frac{\ddot{a}(t)}{a(t)} + \frac{1}{2}\left(\frac{\dot{a}(t)}{a(t)}\right)^2 = -4\pi Gp + \frac{\Lambda}{2} - \frac{1}{2K^2a^2(t)} \quad (3.6.6)$$

By carefully combining equations (3.6.3) and (3.6.6), we can derive an equation that excludes the term  $\left(\frac{\dot{a}}{a}\right)^2$ , making its interpretation more straightforward. Specifically, by performing the operation  $2 \cdot (3.6.6) - (3.6.3)$ , we arrive at:

$$\frac{\ddot{a}(t)}{a(t)} = -\frac{4\pi G}{3}(\rho(t) + 3p) + \frac{\Lambda}{3} \quad (3.6.7)$$

It is noteworthy that there exist only two independent Friedmann equations, with equations (3.6.3) and (3.6.7) serving as our chosen references.

In summary, the Friedmann equations affirm that under general circumstances, the universe is not static.

### 3.7 Number density, Energy density, and Pressure

To understand  $n$ ,  $\rho$ , and  $P$  for various particles in the early universe, we need to know their distribution in phase space. For a homogeneous and isotropic distribution, phase space depends only on absolute value of momentum.

For relativistic particles, the distribution function is given by Bose-Einstein statistics for bosons (-) and Fermi-Dirac statistics for fermions (+). Both can be written as

$$f_{\pm}(p) = \frac{1}{\exp\left(\frac{E-\mu}{T}\right) \pm 1} \quad (3.7.1)$$

At an early time, all particles were in thermal equilibrium with each other i.e., at the same temperature. The chemical potential ( $\mu$ )<sup>1</sup> was small so can be neglected (used  $\mu = 0$ )<sup>2</sup>.

If the internal degree of freedom is  $g$ , particle density in phase space is given by  $g/(2\pi)^3 f(p)$ .

To find number density  $n$ , we integrate particle density over momentum as

$$n = \frac{g}{(2\pi)^3} \int f(p) d^3p \quad (3.7.2)$$

and

---

<sup>1</sup>The chemical potential of a species represents the energy change associated with a variation in the particle number of that species,  $\mu = \delta G / \delta N|_T$ .

<sup>2</sup>Setting  $\mu = 0$  implies that the number of particles and antiparticles are equal, which is not reflective of reality. Therefore, introducing a non-zero  $\mu$  enables us to address the baryon asymmetry. For simplicity in calculations, we adopt  $\mu = 0$ .

$$\rho = \frac{g}{(2\pi)^3} \int E(p) f(p) d^3p \quad (3.7.3)$$

also

$$P = \frac{g}{(2\pi)^3} \int \frac{p^2}{3E(p)} f(p) d^3p \quad (3.7.4)$$

For relativistic case  $E(p) = \sqrt{p^2 + m^2} \approx p$  as  $p \gg m$ .

**For bosons**

$$n_b = \frac{\xi(3)}{\pi^2} gT^3 \quad (3.7.5)$$

$$\rho_b = \frac{\pi^2}{30} gT^4 \quad (3.7.6)$$

**For fermions,**

$$n_f = \frac{3}{4} \frac{\xi(3)}{\pi^2} gT^3 \quad (3.7.7)$$

$$\rho_f = \frac{7}{8} \frac{\pi^2}{30} gT^4 \quad (3.7.8)$$

For a gas filled in container, change in momentum of particle due to collision with walls in x-direction is,  $\delta p = 2p_x$  and total number of particles  $N(p)$  with momentum space  $= n(p)A\delta x$ . So,

$$P = \frac{g}{3(2\pi)^3} \int d^3p f(p) E(p) = \frac{1}{3} \rho \quad (3.7.9)$$

**For non-relativistic particles**

$$E(p) = \sqrt{p^2 + m^2} \approx m + \frac{p^2}{2m} \quad (3.7.10)$$

So

$$n = g \left( \frac{mT}{2\pi} \right)^{\frac{3}{2}} \exp \left( -\frac{m}{T} \right) \quad (3.7.11)$$

also  $\rho = mn$  and  $P = nT$ . Since  $T \ll m$ . So,

$$P \sim 0 \quad (3.7.12)$$

and pressure due to vacuum energy density is,

$$P = -\rho_\nu \quad (3.7.13)$$

So, using equations (3.33), (3.36) and (3.37), we can write a general form for pressure as,

$$P = \omega\rho \quad (3.7.14)$$

Here,  $\omega = 1/3$  for relativistic particles,  $\omega = 0$  for non-relativistic particles and  $\omega = -1$  for vacuum energy. We get total energy density as

$$\rho = \sum_i \frac{\pi^2}{30} g_i T^4 + \frac{7}{8} \sum_j \frac{\pi^2}{30} g_j T^4 = \sum \frac{\pi^2}{30} g_* T^4 \quad (3.7.15)$$

Here,

$$g_* = \sum_i g_i + \frac{7}{8} \sum_j g_j \quad (3.7.16)$$

and  $T$  is the temperature of the photon, which was measured from cosmic microwave background radiation (CMBR) as  $T \approx 2.73$  K. However

because some particle types are no longer in thermal interaction with photons, they may have a different temperature. Neutrinos, for example, essentially separated from other particles before the annihilation of most positrons and electrons into photons. So, at present, neutrino temperature is roughly 1.95 K.

As a result, we can write,

$$g_* = \sum_i g_i \left( \frac{T_i}{T} \right)^4 + \frac{7}{8} \sum_j g_j \left( \frac{T_j}{T} \right)^4 \quad (3.7.17)$$

For the relativistic case we get,

$$3 \frac{\dot{R}}{R} \left( \rho + \frac{\rho}{3} \right) + \dot{\rho} = 0 \quad (3.7.18)$$

On rearranging and integrating, we get

$$\rho \propto \frac{1}{R^4} \quad (3.7.19)$$

$$\frac{\dot{R}^2}{R} \sim \frac{8\pi G}{3R^4} \sim \frac{1}{R^4} \quad (3.7.20)$$

On solving we get,  $R \sim t^{\frac{1}{2}}$ . Hence,

$$H = \frac{\dot{R}}{R} = \frac{1}{2t} \quad (3.7.21)$$

For the non-relativistic case, we get

$$3 \frac{\dot{R}}{R} \rho + \dot{\rho} = 0 \quad (3.7.22)$$

On rearranging and integrating, we get

$$\rho \propto \frac{1}{R^3} \quad (3.7.23)$$

For non-relativistic case, the Friedmann equation can be reduced as

$$R \sim t^{\frac{2}{3}} \quad (3.7.24)$$

So

$$H = \frac{\dot{R}}{R} = \frac{2}{3t} \quad (3.7.25)$$

Event	Time	Temperature
Neutrino decoupling	$\approx 1 \text{ s}$	$\approx 1\text{MeV}$
BBN	$10^1 - 10^3 \text{ s}$	$100\text{keV} - 1\text{keV}$
Recombination	$\approx 300\text{kyr}$	$\approx 0.4\text{eV}$
Baryon acoustic oscillation	$\approx 50\text{kyr} - 350\text{kyr}$	$\approx 0.75\text{eV} - 0.26\text{eV}$
Present	$\approx 13.8\text{Gyr}$	$\approx 10^{-4}\text{eV}$

Table 3.2: Timeline of the expanding universe

Let us go over some of the major epochs one by one.

## 3.8 Entropy

The universe contains significantly more photons than baryons, resulting in the entropy of a uniform universe being predominantly influenced by relativistic particles.

$$dE = TdS - PdV \quad (3.8.1)$$

Here, the change in energy ( $dE$ ) equals the work done changing the volume plus the product of temperature and the change in entropy. In

cosmological terms, where energy ( $E$ ) within a volume ( $V$ ) is represented by  $\rho V$ , we derive:

$$Vd\rho + \rho dV = TdS - PdV \quad (3.8.2)$$

Since  $V \propto a^3$ , the energy conservation equation is

$$\frac{d\rho}{dt} = -3H(\rho + P) = -\frac{1}{V} \frac{dV}{dt}(\rho + P) \quad (3.8.3)$$

so substituting in we have

$$-\frac{dV}{dt}(\rho + P) + \rho \frac{dV}{dt} \quad (3.8.4)$$

$$\implies = T \frac{dS}{dt} - P \frac{dV}{dt} \quad (3.8.5)$$

$$\implies \frac{dS}{dt} = 0 \quad (3.8.6)$$

Therefore, the overall entropy within a comoving volume remains constant, as one would anticipate for a closed system where there are no outlets for heat transfer. Another valuable perspective is to examine the entropy density  $s$ , defined as  $s = S/V$ .

$$T(sdV + Vds) = Vd\rho + \rho dV + PdV \quad (3.8.7)$$

$$\implies d\rho - Tds = (Ts - \rho - P) \frac{dV}{V} \quad (3.8.8)$$

Within the framework of an equilibrium system,  $\rho = \rho(T)$ ,  $s = s(T)$ , and  $P = P(T)$ . Given that  $ds$  and  $d\rho$  are intensive quantities that vary proportionally with  $dT$ , the coefficients associated with the  $dT$  and  $dV$  terms must individually be zero. This condition implies that during a

volume change at constant temperature, the coefficient of the  $dV$  term must be zero.

To derive an expression for the entropy density ( $s$ ) with respect to volume ( $V$ ), we examine the coefficient associated with the  $dV$  term.

$$s = \frac{1}{T}(\rho + P) \quad (3.8.9)$$

The coefficient  $dT$  becomes zero based on the energy conservation equation  $\dot{\rho}$ .

Consequently, we anticipate that  $S \propto a^3 s$  remains conserved across various time periods when a uniform universe is in thermodynamic equilibrium. This principle also holds true for distinct decoupled (non-interacting) components, provided each component individually maintains a thermal distribution with its own temperature.

In the case of a relativistic species  $A$  existing in thermal equilibrium at temperature  $T_A$ , we have previously observed that:

$$\rho_A = g_A^{\text{eff}} \frac{\pi^2}{30} T_A^4 = 3p_A \quad (3.8.10)$$

where  $g_a^{\text{eff}} = g_A$  for bosons, and  $g_a^{\text{eff}} = 7g_A/8$  for fermions. The total entropy density  $s$  is given by:

$$s = \sum_{F,B} s_A(T_A) = \frac{\pi^2}{30} \left(1 + \frac{1}{3}\right) T_\gamma^3 \left[ \sum_B \left(\frac{T_A}{T_\gamma}\right)^3 + \frac{7}{8} \sum_F \left(\frac{T_A}{T_\gamma}\right)^3 \right] \quad (3.8.11)$$

$$= \frac{2\pi^2}{45} g_{*S} T_\gamma^3, \quad (3.8.12)$$

In the context where  $T_\gamma$  represents the temperature of photons, the effective number of degrees of freedom in entropy is defined by:

$$g_{*S} = \sum_B \left( \frac{T_A}{T_\gamma} \right)^3 + \frac{7}{8} \sum_F \left( \frac{T_A}{T_\gamma} \right)^3 \quad (3.8.13)$$

It's important to highlight that  $g_{*S}$  equals  $g_*$  only under the condition that all relativistic species are in equilibrium at the same temperature.

Applying the conservation of entropy, we can express this relationship as follows:

$$d(g_{*S}a^3T^3) = 0 \Rightarrow T \propto g_{*S}^{-1/3}a^{-1} \quad (3.8.14)$$

## Decoupling

To achieve equilibrium within a system, the constituent particles must engage in frequent interactions, exchanging energy and momentum. For any given particle species (or pair of species), we can quantify the interaction rate  $\Gamma$ . The characteristic time for a particle to interact with another is defined as  $t_{\text{int}} = 1/\Gamma$ . It becomes meaningful to discuss equilibrium as long as the universe remains relatively unchanged within the timescale  $t_{\text{int}}$ . Considering the universe's expansion governed by the Hubble parameter  $H$ , we can establish equilibrium under the condition:

$$\Gamma \gg H \quad (3.8.15)$$

Conversely, if  $\Gamma \ll H$ , significant expansion of the universe occurs by the time particles interact, leading to an inability to maintain thermal equilibrium.

For many processes, the interaction rate and Hubble rate scale proportionally with  $T$  (temperature), albeit in distinct manners. As a consequence, particles can remain in equilibrium during early times but eventu-

ally decouple from the thermal bath as time progresses. This decoupling phase, occurring when  $\Gamma \approx H$ , is called *freeze-out*.

Interaction and Hubble rates are given by

$$\Gamma = n\langle\sigma v\rangle \quad \text{and} \quad H = \sqrt{\frac{8\pi G}{3c^2}\rho} \quad (3.8.16)$$

where  $\langle\sigma v\rangle$  is the thermally averaged cross section,  $n$  is the number density of the DM and  $\rho$  is the energy density of the DM.

### 3.9 Neutrino decoupling

At temperatures below  $T \simeq 10^{12}$  K  $\simeq O(100)$ MeV, the dominant energy density in the universe is primarily attributed to relativistic particles such as  $e^\pm$ ,  $\nu$ ,  $\bar{\nu}$ , and photons. Given that these particles are in thermal equilibrium at this temperature, the effective no. of degrees of freedom is  $g_* = 10.75$ . During this radiation-dominated epoch, the rate of expansion is described by:

$$H(T) = \frac{\sqrt{8\pi\rho_R}^{1/2}}{\sqrt{3}m_P} \simeq 5.44 \frac{T^2}{m_P} \quad (3.9.1)$$

Neutrinos remains in equilibrium through weak interaction ( $\bar{\nu}\nu \leftrightarrow e^+e^-, \dots$ ), with a cross section:

$$\sigma_F \simeq G_F^2 E^2 \simeq G_F^2 T^2 \quad (3.9.2)$$

where  $G_F$  is the Fermi constant which equals to  $1.1664 \times 10^{-5}\text{GeV}^{-2}$ . The interaction rate per (massless) neutrino is:

$$\Gamma_F \simeq 1.3G_F^2 T^5 \quad (3.9.3)$$

and

$$\frac{\Gamma_F}{H(T)} \simeq 0.24T^3 G_F^2 m_P \simeq \left( \frac{T}{1\text{MeV}} \right)^3 \quad (3.9.4)$$

Therefore, neutrinos cease to interact significantly with other matter at a temperature approximately around  $T_D \simeq 1\text{MeV}$ . Below  $1\text{MeV}$ , the temperature of neutrinos decreases with the scale factor  $a^{-1}$ . Shortly after neutrino decoupling, when the temperature falls below the electron mass ( $T < 0.5\text{MeV}$ ), the entropy stored in electron-positron pairs is transferred to photons, but not to neutrinos. This scenario can be described by the following equations:

$$g_* = 2 + \frac{7}{8}4 = \frac{11}{2}, \quad g_*(T < m_e) = 2 \quad (3.9.5)$$

The principle of entropy conservation, given by  $S = g_* S(aT)^3$  for particles in equilibrium with radiation, indicates that the quantity  $g_* S(T_\gamma a)^3 = g_*(T_\gamma a)^3$  remains unchanged during expansion. As  $g_*$  decreases following  $T < m_e$ , the value of  $(aT_\gamma)^3$  becomes larger after electron-positron ( $e^- e^+$ ) annihilation compared to its value prior to this event.

$$\frac{(aT_\gamma)_{\text{after}}^3}{(aT_\gamma)_{\text{before}}^3} = \frac{(g_*)_{\text{before}}}{(g_*)_{\text{after}}} = \frac{11}{4} \quad (3.9.6)$$

Neutrinos do not participate in this process, and their entropy is independently preserved. However, prior to the initiation of  $e\bar{e}$  annihilation, photons and neutrinos shared the same temperature. Therefore

$$(aT_\gamma)_{\text{after}} = \left( \frac{11}{4} \right)^{1/3} (aT_\nu)_{\text{after}} \quad (3.9.7)$$

Today, the temperature of photons ( $T_{\gamma 0} = 2.726$  K) is higher than that of neutrinos by a factor of  $(11/4)^{1/3} \sim 1.4$  (thus,  $T_{\nu 0} \sim 1.92$  K). Because  $T_{\gamma} \neq T_{\nu}$ , the effective number of relativistic degrees of freedom today, denoted as  $g_*$ , differs from the number of entropy degrees of freedom, denoted as  $g_{*S}$ . Specifically, we have  $g_* \simeq 3.36$  and  $g_{*S} \simeq 3.91$ .

## 3.10 Big Bang Nucleosynthesis

One of the most comprehensively understood phenomena within the Big Bang fireball is the process by which deuterium, helium, and heavier nuclei are formed from the thermal pool of protons and neutrons. Referred to as Big Bang nucleosynthesis, this intricate calculation draws upon various branches of physics. Despite the potential for discrepancies, the outcome aligns seamlessly with the observed abundance of light elements. This success stands as a notable achievement of the Big Bang theory.

### 3.10.1 Neutrons and Protons

The narrative begins in the early universe, at times much less than one second ( $t \ll 1$  second), when the temperature soared to values where  $k_B T \gg 1$  MeV. The mass of the electron is

$$m_e c^2 \approx 0.5 \text{ MeV} \tag{3.10.1}$$

At this juncture, the thermal environment consists of numerous relativistic electron-positron pairs. These pairs are in a state of equilibrium with photons and neutrinos, all of which are relativistic, alongside non-relativistic protons and neutrons. This equilibrium is sustained by interactions facilitated by the weak nuclear force.

$$n + \nu_e \leftrightarrow p + e^-, \quad n + e^+ \leftrightarrow p + \bar{\nu}_e \quad (3.10.2)$$

The chemical potentials of electrons and neutrinos are extremely small. In order to maintain chemical equilibrium, it follows that  $\mu_n = \mu_p$ , allowing us to calculate the ratio of neutron to proton densities in a non-relativistic gas.

$$\frac{n_n}{n_p} = \left( \frac{m_n}{m_p} \right)^{3/2} e^{-\beta(m_n - m_p)c^2} \quad (3.10.3)$$

The proton and neutron exhibit an extremely slight disparity in mass,

$$\begin{aligned} m_n c^2 &\approx 939.6 \text{ MeV} \\ m_p c^2 &\approx 938.3 \text{ MeV} \end{aligned} \quad (3.10.4)$$

The difference in mass can be disregarded in the prefactor, yet it plays a critical role in the exponent. This determines the ratio of protons to neutrons during equilibrium.

$$\frac{n_n}{n_p} \approx e^{-\beta \Delta m c^2} \quad \text{with} \quad \Delta m c^2 \approx 1.3 \text{ MeV} \quad (3.10.5)$$

When the temperature  $k_B T$  is significantly greater than the mass difference  $\Delta m c^2$ , the numbers of protons and neutrons are roughly equal. However, as the temperature decreases, the number of neutrons also decreases.

The exponential decline in the neutron count does not continue indefinitely. Eventually, the rate of weak interactions will decrease to a point where  $\Gamma \sim H$ , leading to neutron freeze-out and a constant neutron number. Neutrons are predicted to decouple at a specific temperature.

$$k_B T_{\text{dec}} \approx 0.8 \text{ MeV} \quad (3.10.6)$$

Utilizing  $g_\star \approx 3.4$ , it is determined that neutrons decouple at

$$t_{\text{dec}} \approx 2 \text{ seconds} \quad (3.10.7)$$

At the point of freeze-out, we are consequently left with a neutron-to-proton ratio of

$$\frac{n_n}{n_p} \approx \exp\left(-\frac{1.3}{0.8}\right) \approx \frac{1}{5} \quad (3.10.8)$$

Indeed, the narrative doesn't conclude here. Neutrons, if left undisturbed, exhibit instability through beta decay with a half-life slightly exceeding 10 minutes. Consequently, following freeze-out, the number density of neutrons undergoes decay according to the equation

$$n_n(t) \approx \frac{1}{5} n_p(t_{\text{dec}}) e^{-t/\tau_n} \quad (3.10.9)$$

where  $\tau_n \approx 880$  second.

### 3.10.2 Deuterium

Ultimately, our goal is to synthesize elements heavier than hydrogen. However, these heavier nuclei typically contain more than two nucleons. For instance, the lightest of these nuclei is  $^3\text{He}$ , composed of two protons and one neutron. The probability of three particles simultaneously colliding to form such a nucleus is exceedingly low. Therefore, we must proceed incrementally, gradually building up these nuclei through pairwise collisions.

The initial step in this process happens to be the most challenging. This step involves the formation of deuterium, also known as heavy hydrogen, which is a bound state of a proton and a neutron. This state is achieved through the reaction



The binding energy is

$$E_{\text{bind}} \approx 2.2\text{MeV} \quad (3.10.11)$$

Both the proton and neutron possess a spin of  $1/2$ , resulting in identical gyromagnetic ratios:  $g_n = g_p = 2$ . Within deuterium, the spins align to create a composite spin-1 particle, leading to a gyromagnetic ratio of  $g_D = 3$ . The proportion of deuterium can subsequently be calculated using the Saha equation, employing similar principles to those utilized in recombination.

$$\frac{n_D}{n_n n_p} = \frac{3}{4} \left( \frac{m_D}{m_n m_p} \frac{2\pi\hbar^2}{k_B T} \right)^{3/2} e^{\beta E_{\text{bind}}} \quad (3.10.12)$$

Approximating  $m_n \approx m_p \approx \frac{1}{2}m_D$

$$\frac{n_D}{n_p} \approx \frac{3}{4} n_n \left( \frac{4\pi\hbar^2}{m_p k_B T} \right)^{3/2} e^{\beta E_{\text{bind}}} \quad (3.10.13)$$

We will make a straightforward estimation of the number of neutrons using the following approximation:

$$n_n \approx n_p \approx \eta n_\gamma \quad (3.10.14)$$

The ratio of baryons to photons,  $\eta$ , has remained approximately constant since nucleosynthesis up to the present day, with  $\eta \approx 10^{-9}$ . The last significant change occurred during the annihilation of electrons and positrons, represented by the reaction  $e^- + e^+ \rightarrow \gamma + \gamma$ . Utilizing the expression for

the number density of photons,  $n_\gamma \approx (k_B T/c)^3$ , we can then express

$$\frac{n_D}{n_p} \approx \eta \left( \frac{k_B T}{m_p c^2} \right)^{3/2} e^{\beta E_{\text{bind}}} \quad (3.10.15)$$

We observe that a significant number of deuterium atoms only form when the temperature decreases to a sufficiently low level. This delay in deuterium formation is primarily attributed to the abundance of photons, as indicated by the factor  $\eta$ . These photons, which are numerous at this stage, also contribute to the delayed formation of hydrogen 300,000 years later. In both scenarios, any potential bound state is quickly disrupted by the bombardment of high-energy photons from the tail end of the blackbody distribution.

Solving the equation, we find that  $n_D/n_p \sim 1$  only when  $\beta E_{\text{bind}} \approx 35$ , or

$$k_B T \lesssim 0.06 \text{ MeV} \quad (3.10.16)$$

Significantly, this occurs following the decoupling of neutrinos. Once more, with  $g_\star \approx 3.4$ , we observe the initiation of deuterium formation at

$$t \approx 360 \text{ seconds} \quad (3.10.17)$$

Approximately six minutes after the Big Bang, a crucial window of time opens up. Fortunately, this timeframe is still within the 10.5 minutes required for neutrons to decay. However, the situation becomes increasingly precarious. If the specifics were altered such that, for instance, it took 12 minutes instead of 6 for deuterium to form, our existence today would be in jeopardy. The creation of a universe, it appears, demands precision and delicacy.

### 3.10.3 Helium and Heavier Nuclei

The binding energy for  ${}^3\text{He}$  is  $7.7\text{MeV}$ , whereas for  ${}^4\text{He}$  it is  $28\text{MeV}$ . Once deuterium is present, however, there are no obstacles to the formation of helium. This occurs almost instantaneously through



Due to the significantly higher binding energy, all remaining neutrons quickly combine to form  ${}^4\text{He}$  nuclei.

$$\frac{n_n}{n_p} = \frac{1}{5} e^{-360/880} \approx 0.13 \quad (3.10.19)$$

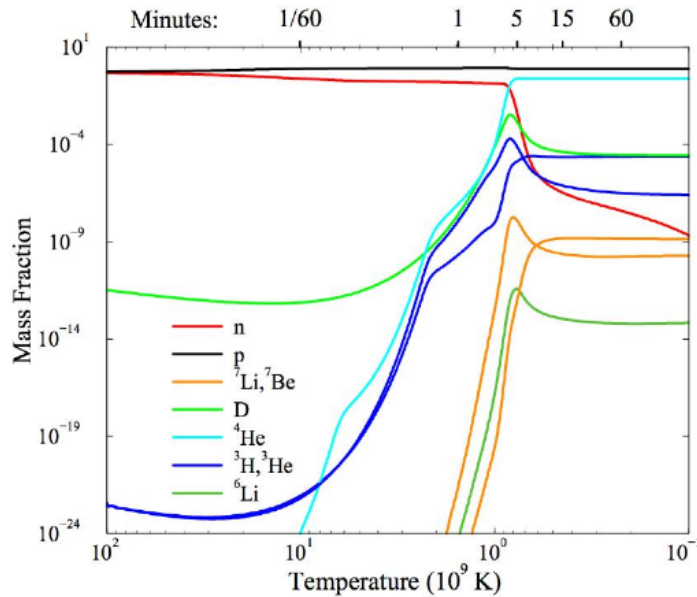


Figure 3.2: The presence of light nuclei in the early universe

Given that each  ${}^4\text{He}$  atom consists of two neutrons, the ratio of helium to hydrogen is expressed as

$$\frac{n_{\text{He}}}{n_{\text{H}}} = \frac{n_n/2}{n_p - n_n} \approx 0.07 \quad (3.10.20)$$

A helium atom is approximately four times more massive than a hydrogen atom, indicating that roughly 25% of the baryonic mass is composed of helium, with the remainder being hydrogen. This proportion closely matches the observed abundance in the universe. Even smaller quantities of  ${}^7\text{Li}$  and  ${}^7\text{Be}$  are present, all consistent with observational data. [6]

Figure 3.2<sup>3</sup> illustrates the time-dependent abundance of various elements. The red neutron curve demonstrates a decline as neutrons decay, while the abundance of other elements rises, indicating the resolution of the deuterium bottleneck over time.

### 3.11 Recombination

We are interested in studying a system of electrons and protons in thermal equilibrium at a certain temperature. These particles have the capability to combine and produce hydrogen, a process we will liken to atomic reactions similar to chemical reactions.



The inquiry we wish to pose is: what fraction of the particles consist of hydrogen, and what fraction consist of electron-proton pairs?

We will hypothesize that the hydrogen atom is formed in its lowest energy state, characterized by a binding energy

$$E_{\text{bind}} \approx 13.6\text{eV} \tag{3.11.2}$$

At first glance, one might expect hydrogen to ionize once temperatures reach around  $k_B T \approx E_{\text{bind}}$ . Indeed, at temperatures where  $k_B T \gg E_{\text{bind}}$ ,

---

<sup>3</sup>This figure is taken from Burles, Nollett and Turner, Big-Bang Nucleosynthesis, astro-ph/99033.

electrons cannot effectively remain bound to protons, resulting in the breakup of hydrogen atoms. However, it turns out that hydrogen formation occurs at temperatures significantly lower than  $E_{\text{bind}}$ .

To analyze this scenario, we approach each massive particle - the electron, proton, and hydrogen atom - similarly to a non-relativistic gas. Initially, we consider the rest mass energy of these particles, ensuring that each particle possesses energy.

$$E_{\mathbf{p}} = mc^2 + \frac{p^2}{2m} \quad (3.11.3)$$

This will be valuable because we can consider the binding energy  $E_{\text{bind}}$  as equivalent to the mass difference

$$E_{\text{bind}} \approx 13.6\text{eV} \quad (3.11.4)$$

Next, each of the particle is associated with a number  $g$  representing its internal states. Both electron and proton possess  $g_e = g_p = 2$ , corresponding to two spin states known as “spin up” and “spin down.” This concept is akin to the two polarization states of the photon discussed earlier in the context of blackbody radiation. For hydrogen (H), the value is  $g_H = 4$ ; the alignment of electron and proton spins can result in a spin-0 particle or three distinct spin-1 states.

Incorporating these adjustments, the expression for the number density of various particle species is as follows:

$$n_i = g_i \left( \frac{m_i k_B T}{2\pi \hbar^2} \right)^{3/2} e^{-\beta(m_i c^2 - \mu_i)} \quad (3.11.5)$$

It is essential that these particles maintain chemical equilibrium, indicating a steady state where rapid transitions between  $e^- + p^+$  pairs and

hydrogen do not occur. This equilibrium is maintained by ensuring that the chemical potentials are interconnected according to

$$\mu_e + \mu_p = \mu_H \quad (3.11.6)$$

Photons do not possess a chemical potential because they are not conserved particles. Specifically, in addition to the reaction  $e^- + p^+ \leftrightarrow H + \gamma$ , there are reactions where the resulting binding involves two photons, such as  $e^- + p^+ \leftrightarrow H + \gamma + \gamma$ . This illustrates why discussing a chemical potential for photons is nonsensical.

To eliminate the chemical potentials and establish equilibrium conditions, we can apply the following equation:

$$\frac{n_H}{n_e n_p} = \frac{g_H}{g_e g_p} \left( \frac{m_H}{m_e m_p} \frac{2\pi\hbar^2}{k_B T} \right)^{3/2} e^{-\beta(m_H - m_e - m_p)c^2} \quad (3.11.7)$$

In the pre-factor, it is reasonable to approximate  $m_H \approx m_p$ . However, in the exponent, the distinction between these masses is critical; it represents the binding energy of hydrogen. Lastly, we incorporate the observed condition that the universe is electrically neutral, thus

$$n_e = n_p \quad (3.11.8)$$

We have

$$\frac{n_H}{n_e^2} = \left( \frac{2\pi\hbar^2}{m_e k_B T} \right)^{3/2} e^{\beta E_{\text{bind}}} \quad (3.11.9)$$

This is the Saha equation. Here we introduce the ionization fraction

$$X_e = \frac{n_e}{n_B} \approx \frac{n_e}{n_p + n_H} \quad (3.11.10)$$

in the second equality of the equation, we are excluding neutrons and heavier elements. When  $n_e = n_p$ , a value of  $X_e = 1$  signifies that all electrons are unbound. Conversely, if  $X_e = 0.1$ , it indicates that only 10% of the electrons are not bounded within the hydrogen, while the rest are bound within hydrogen.

Utilizing the condition  $n_e = n_p$ , we derive  $1 - X_e = n_H/n_B$ , thereby obtaining

$$\frac{1 - X_e}{X_e^2} = \frac{n_H}{n_e^2} n_B \quad (3.11.11)$$

To convert this into the fraction  $X_e$ , we also require knowledge of the total number of baryons, which we derive from observational data.

$$\eta = \frac{n_B}{n_\gamma} \approx 10^{-9} \quad (3.11.12)$$

Here we utilize the constant value of  $\eta \approx 10^{-9}$  since recombination. Following this, we leverage the equilibrium condition where photons share the same temperature as electrons, protons, and hydrogen. Consequently, we can apply our previously derived expression for the number of photons.

$$n_\gamma = \frac{2\zeta(3)}{\pi^2 \hbar^3 c^3} (k_B T)^3 \quad (3.11.13)$$

Combining these gives our final answer

$$\frac{1 - X_e}{X_e^2} = \eta \frac{2\zeta(3)}{\pi^2} \left( \frac{2\pi k_B T}{m_e c^2} \right)^{3/2} e^{\beta E_{\text{bind}}} \quad (3.11.14)$$

Let's consider the temperature  $k_B T \sim E_{\text{bind}}$ , which is typically where we might expect recombination to occur. In this scenario, we encounter two very small quantities at play: the factor  $\eta \sim 10^{-9}$  and  $k_B T/m_e c^2$ , where the electron mass  $m_e c^2 \approx 0.5 \text{ MeV} = 5 \times 10^5 \text{ eV}$ . These factors ensure

that at  $k_B T \sim E_{\text{bind}}$ , the ionization fraction  $X_e$  remains very close to unity. Essentially, this implies that almost all electrons remain free and unbound, primarily due to the abundance of photons. Even when a proton and electron combine, there are still enough high-energy photons in the blackbody distribution tail to break them apart.

Recombination occurs when the factor  $e^{\beta E_{\text{bind}}}$  is sufficient to counterbalance both  $\eta$  and  $k_B T/m_e c^2$ . Recombination is not a singular event; it happens continuously as the temperature changes. As an illustrative example, let's calculate the temperature at which  $X_e = 0.1$ , indicating that 90% of electrons have combined with protons to form hydrogen. We find that this occurs when  $\beta E_{\text{bind}} \approx 45$ , or

$$k_B T_{\text{rec}} \approx 0.3\text{eV} \quad \Rightarrow \quad T_{\text{rec}} \approx 3600 \text{ K} \quad (3.11.15)$$

This corresponds to a redshift of

$$z_{\text{rec}} = \frac{T_{\text{rec}}}{T_0} \approx 1300 \quad (3.11.16)$$

This occurs much later than matter-radiation equality, which happens at  $z_{\text{eq}} \approx 3400$ . Consequently, during recombination, the universe is dominated by matter, where  $a(t) \sim (t/t_0)^{2/3}$ . Therefore, we can assign the time of recombination to

$$t_{\text{rec}} \approx \frac{t_0}{(1 + z_{\text{rec}})^{3/2}} \approx 300,000 \text{ years} \quad (3.11.17)$$

Following recombination, the components of the universe primarily consist of neutral atoms. In simple terms, this indicates that the universe has become transparent, allowing photons to propagate freely.

## 3.12 Baryon acoustic oscillations

In the early universe, there exists a period delineated by redshifts[3]

$$1100 \lesssim z \lesssim 3400 \tag{3.12.1}$$

when cosmic expansion was mostly dominated by matter, but before hydrogen had formed, protons, electrons, and photons existed in a state of thermal equilibrium. In the photon-baryon fluid described here, the speed of sound is predominantly governed by photons rather than matter, resulting in  $c_s \approx c/\sqrt{3}$ .

As a result, dark matter and baryonic matter exhibit distinct behaviors during this epoch. Density perturbations in dark matter, having decoupled from photons long ago, begin to grow as  $\delta \sim a$ . Meanwhile, density perturbations in baryonic matter are influenced by photon pressure and, particularly on subhorizon scales, undergo oscillations. These oscillations within the baryon-photon fluid are commonly referred to as baryonic acoustic oscillations.

Two significant consequences arise from this scenario. Firstly, dark matter gains an early advantage in structure formation, initiating density perturbations that commence growth around  $z \approx 3400$ . By the time baryons decouple at  $z = 1100$ , gravitational wells have already formed, serving as seeds that accelerate the formation of baryonic structures, including galaxies.

The second consequence is more nuanced. During recombination, photons disperse away from the sound waves they previously influenced. Meanwhile, the baryons remain fixed in position, retaining a snapshot of their earlier state. These sound waves exhibit areas of baryonic compression and rarefaction, with their wavelengths determined by the horizon at decoupling.

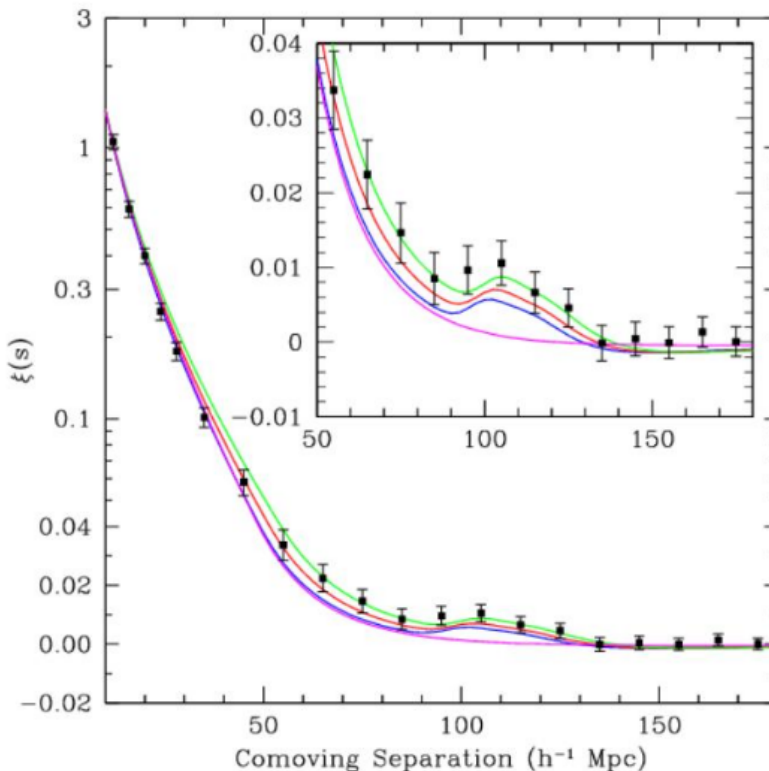


Figure 3.3: Baryonic acoustic oscillations observed in the galaxy distribution. [7]

$$d_H \sim \frac{cH_0^{-1}}{(1+z)^{3/2}} \approx 0.1\text{Mpc} \quad (3.12.2)$$

Employing  $cH_0^{-1} \approx 4 \times 10^3\text{Mpc}$  and  $z \approx 1100$ , these waves underwent significant stretching during the subsequent evolution of the universe, scaling up by a factor of  $z \approx 1100$ . This stretching left a subtle mark on the clustering of matter observed today, notably reflected in an excess of galaxies spaced approximately  $\sim 150\text{Mpc}$  apart. The presence of these baryonic acoustic oscillations in the galaxy distribution was initially detected in 2005; the correlation function is shown in Figure 3.3<sup>4</sup>.

---

<sup>4</sup>This data is taken from D. J. Eisenstein et al. [SDSS Collaboration], “Detection of the Baryon Acoustic Peak in the Large-Scale Correlation Function of SDSS Luminous Red Galaxies” *Astrophys. J.* 633, 560 (2005), astro-ph/0501171.

## Chapter 4

# Detection prospects of CNB at PTOLEMY

The current temperature of relic neutrinos from the Cosmic Neutrino Background (CNB) is  $T_{\nu,0} = 1.945$  Kelvin, rendering them highly non-relativistic and lacking sufficient energy to be detected by conventional neutrino experiments. A compelling approach to detect these relic neutrinos involves neutrino capture on  $\beta$ -unstable nuclei. This method offers a significant advantage in that it does not require a threshold energy for the initial state neutrinos.

Building upon this concept, the PTOLEMY [2] experiment is proposed to utilize tritium ( ${}^3H$ ) as the target element, offering optimal conditions for CNB detection due to its favorable lifetime, availability, low Q value, and high neutrino capture cross-section. The process of neutrino capture on  ${}^3H$  is described by the equation:



## 4.1 Neutrino capture by neutron

We begin by examining the scenario involving the fundamental process of neutrino scattering with a neutron, and then extend our discussion to encompass the case involving tritium.

$$\nu_j + n \rightarrow p + e^- \quad (4.1.1)$$

Given the modest energy scales involved, we can confidently operate within the framework of the four-fermion interaction approximation, enabling us to derive the following equations: [1]

$$iM_j = -i\frac{G_F}{\sqrt{2}}V_{ud}U_{ej}^*[\bar{u}_e\gamma^\alpha(1-\gamma^5)u_{\nu_j}][\bar{u}_p\gamma^\beta(f(0)-g(0)\gamma^5)u_n]\eta_{\alpha\beta} \quad (4.1.2)$$

In the context provided, where  $u_x$  represents the Dirac spinor for  $x$  and  $V_{ud} = 0.97425$  is an element of CKM matrix, the presence of the element  $U_{ej}$  within the PMNS matrix is due to the involvement of only the electron component from each mass eigenstate in the process. The functions  $f(q)$  and  $g(q)$  denote nuclear form factors, with  $f \equiv f(0) \approx 1$  and  $g \equiv g(0) \approx 1.2695$  in the limit of small transfer of momentum.

The next step involves calculating the cross section by squaring the amplitude and performing the necessary spin sums, as detailed in Appendix A.

$$\overline{|M_j|^2}(s_\nu) = 8G_F^2|V_{ud}|^2|U_{ej}|^2m_n m_p E_e E_\nu [A(s_\nu)(f^2 + 3g^2) + B(s_\nu)(f^2 - g^2) v_e \cos\theta] \quad (4.1.3)$$

The spin-dependent factors are:

$$A(s_\nu) \equiv 1 - 2s_\nu v_{\nu j} = \begin{cases} 1 - v_{\nu j}, & s_\nu = +1/2 \quad \text{right helical} \\ 1 + v_{\nu j}, & s_\nu = -1/2 \quad \text{left helical,} \end{cases} \quad (4.1.4)$$

$$B(s_\nu) \equiv v_{\nu j} - 2s_\nu = \begin{cases} v_{\nu j} - 1, & s_\nu = +1/2 \quad \text{right helical} \\ v_{\nu j} + 1, & s_\nu = -1/2 \quad \text{left helical} \end{cases} \quad (4.1.5)$$

If the neutrinos were moving at relativistic speeds, denoted by  $v_{\nu j} \simeq 1$ , then we would determine that  $A = B = 0$  for right-helical neutrinos, indicating that these particles cannot be captured. Conversely, for left-helical neutrinos, we find  $A = B = 2$ . This outcome reflects the well-known result that in the relativistic limit, helicity aligns with chirality, and only left-chiral neutrinos interact via the weak force.

In the non-relativistic regime, pertinent to this context, we observe  $A(\pm 1/2) = \mp B(\pm 1/2) = 1$ , which implies that both left- and right-helical neutrinos can potentially be captured.

We compute the differential cross section by evaluating the squared amplitude using conventional methods.

$$\frac{d\sigma}{d \cos \theta} = \frac{1}{32\pi} \frac{1}{m_n^2} \frac{|p_e|}{|p_\nu|} \overline{|M|^2} \quad (4.1.6)$$

$$\frac{d\sigma_j(s_\nu)}{d \cos \theta} = \frac{G_F^2}{4\pi} |V_{ud}|^2 |U_{ej}|^2 F(Z, E_e) \frac{m_p E_e p_e}{m_n v_{\nu j}} [A(s_\nu)(f^2 + 3g^2) + B(s_\nu)(f^2 - g^2) v_e \cos \theta] \quad (4.1.7)$$

The Fermi function  $F(Z, E_e)$  accounts for the enhancement of the cross section resulting from the Coulombic attraction between the outgoing electron

and proton. This function can be expressed as

$$F_Z(E_e) = \frac{2\pi Z\alpha E_e/p_e}{1 - \exp(-2\pi Z\alpha E_e/p_e)}. \quad (4.1.8)$$

$Z$ , representing the atomic number of the daughter nucleus (where  $Z = 1$  in this context), and  $\alpha \approx 1/137.036$ , denoting the fine structure constant, are essential parameters in this scenario.

Given that the incoming neutrino is nearly stationary ( $p_\nu \ll p_e$ ), the kinematics permit isotropic emission of the electron. Consequently, integrating over  $\theta$  becomes straightforward, yielding the total capture cross section multiplied by the neutrino velocity. This quantity is crucial for determining the capture rate. [4]

$$\sigma_j(s_\nu)v_{\nu j} = \frac{G_F^2}{2\pi}|V_{ud}|^2|U_{ej}|^2 F(Z, E_e) \frac{m_p}{m_n} E_e p_e A(s_\nu)(f^2 + 3g^2) \quad (4.1.9)$$

Given that  $A(\pm 1/2) = 1$  under the approximation  $v_{\nu j} \ll 1$ , the cross section remains the same for both spin states. Consequently, any variations in the capture rate among different spin states must originate from their respective abundances in the present era.

## 4.2 Neutrino absorption by tritium

Finally, let us extend our findings to the process



The computation of the cross section follows a similar process to the deriva-

tion of Eq. 4.1.9, with the substitution of  $n \rightarrow {}^3H$  and  $p \rightarrow {}^3He$ . Instead of using the masses of neutrons and protons, we utilize the nuclear masses of the respective isotopes:  $m_n \rightarrow m_{{}^3H} \approx 2808.92$  MeV and  $m_p \rightarrow m_{{}^3He} \approx 2808.39$  MeV.

Instead of using the form factors  $f(q)$  and  $g(q)$ , the focus shifts to nuclear matrix elements. This involves substituting  $f^2$  with  $\langle f_F \rangle^2 \approx 0.9987$  and  $3g^2$  with  $(g_A/g_V)^2 \langle g_{GT} \rangle^2$ , where  $\langle g_{GT} \rangle^2 \approx 2.788$ ,  $g_A \approx 1.2695$ , and  $g_V \approx 1$ . [15].

Upon implementing the substitutions as detailed earlier, we derive the capture cross section times velocity for the mass eigenstate  $j$ :

$$\sigma_j(s_\nu)v_{\nu j} = A(s_\nu)|U_{ej}|^2\bar{\sigma}, \quad (4.2.2)$$

where<sup>1</sup>

$$\bar{\sigma} \equiv \frac{G_F^2}{2\pi}|V_{ud}|^2 F(Z, E_e) \frac{m_{{}^3He}}{m_{{}^3H}} E_e p_e (\langle f_F \rangle^2 + (g_A/g_V)^2 \langle g_{GT} \rangle^2) \simeq 3.834 \times 10^{-45} \text{ cm}^2 \quad (4.2.3)$$

Moving forward, we can now compute the total capture rate anticipated in tritium with mass  $M_T$ . In Equation 4.2.2, the capture cross section is specified for a given neutrino mass and helicity eigenstate. This involves summing the cross section over each of the six initial states, weighted by the corresponding flux:

$$\Gamma_{C\nu B} = \sum_{j=1}^3 [\sigma_j(+1/2)v_{\nu j}n_j(\nu_{hR}) + \sigma_j(-1/2)v_{\nu j}n_j(\nu_{hL})N_T], \quad (4.2.4)$$

---

<sup>1</sup>The calculation is in the mathematica file here: <https://shorturl.at/fixAO>

The quantity  $N_T = M_T/m_{3H}$  represents the approximate number of nuclei in the sample. Utilizing Equation 4.2.2, we can express the capture rate as:

$$\Gamma_{C\nu B} = \sum_{j=1}^3 |U_{ej}|^2 \bar{\sigma} [n_j(\nu_{hR}) + n_j(\nu_{hL}) N_T] = \bar{\sigma} [n(\nu_{hR}) + n(\nu_{hL})] N_T \quad (4.2.5)$$

In this context, the value of  $\bar{\sigma}$  was determined by the equation referenced as eq. 4.1.13. Additionally, under the non-relativistic approximation, we approximated  $A(-1/2) \approx A(+1/2) \approx 1$ .

If the neutrinos are Dirac particles, we saw that  $n(\nu_{hL}) = n_0$  and  $n(\nu_{hR}) = 0$ , and the capture rate becomes[10]

$$\Gamma_{C\nu B}^D = \bar{\sigma} n_0 N_T. \quad (4.2.6)$$

and for Majorana case we get  $n(\nu_{hL}) = n(\nu_{hR}) = n_0$ , and the capture rate becomes

$$\Gamma_{C\nu B}^M = 2\bar{\sigma} n_0 N_T \quad (4.2.7)$$

The capture rate in the Majorana case is twice that in the Dirac case:

$$\Gamma_{C\nu B}^M = 2\Gamma_{C\nu B}^D. \quad (4.2.8)$$

The concept can be elucidated as follows. In the case of Dirac neutrinos, it is determined that the Cosmic Neutrino Background (CνB) comprises solely of left-handed neutrinos and right-handed anti-neutrinos. In the relativistic limit, where helicity and chirality coincide, only the left-handed states can participate in weak interactions. The right-handed states become sterile, resulting in only half of the background neutrinos being available for capture. However, given that the CνB is non-relativistic,

both left-handed and right-handed states possess some left-chiral component, allowing for interaction with weak forces. The right-handed anti-neutrinos remain uncapturable due to the kinematical restriction of the process  $\bar{\nu} + p \rightarrow n + e^+$ , as outlined by Lazauskas et al. (2007) [8]. Consequently, in the Dirac scenario, only half of the  $C\nu B$  abundance is accessible for capture. Conversely, in the Majorana case, no distinction is made between neutrinos and anti-neutrinos. Instead, it is established that the  $C\nu B$  comprises left-handed neutrinos and right-handed neutrinos, both of which interact weakly and therefore are available for capture.

### 4.3 Results

Considering a tritium mass of 100gm, as is proposed for PTOLEMY, eqs. 4.2.6 and 4.2.7 evaluate to

$$\Gamma_{C\nu B}^D \approx 4.06yr^{-1} \quad \text{and} \quad \Gamma_{C\nu B}^M \approx 8.12yr^{-1} \quad (4.3.1)$$

for Dirac and Majorana neutrino cases, respectively. These rates are constrained solely by the size of the sample, as they are unaffected by the neutrino mass (assuming the neutrinos are non-relativistic), and the flux of Cosmic Neutrino Background ( $C\nu B$ ) neutrinos remains constant.

# Chapter 5

## Dark matter particle

### 5.1 WIMP Dark Matter

WIMP, short for Weakly Interactive Massive Particle, represents the primary contemporary model for elucidating the universe's dark matter. The concept of WIMP is straightforward: it denotes a relatively heavy elementary particle denoted by  $\chi$ , beyond the reach of current accelerator experiments due to its mass exceeding  $10^2$  GeV. However, during the early stages of the Big Bang, sufficient energy existed to generate these particles.

Let's trace back to the epoch when the temperature  $T$  surpassed the mass of the WIMP, denoted as  $m_\chi$ . At this juncture, WIMPs were generated alongside other particles. As the temperature dropped below  $m_\chi$ , the universe ceased producing them. Assuming WIMPs are stable, any initially produced particles persisted, with annihilation among themselves into standard particles (e.g., quarks, leptons, gauge bosons) serving as the sole means of diminishing their numbers. However, with the universe's expansion, the density of WIMPs per unit volume steadily declined. Consequently, WIMPs eventually became too sparse to encounter one another, halting their annihilation and fixing their abundance through a process known as "freeze out". This thermal relic mechanism thus accounts for the residual presence of dark matter in the universe. [11]

### 5.1.1 Boltzmann Equation

We postulate kinetic equilibrium, meaning that each particle species conforms to a Boltzmann distribution in momentum space, with the exception of the overall normalization determined by its number density. Considering the process  $\chi_1\chi_2 \leftrightarrow \chi_3\chi_4$ , where  $\chi_i$  represents a specific elementary particle, the Boltzmann equation governing the number density  $n_1$  of particle  $\chi_1$  is [9]

$$a^{-3} \frac{d(n_1 a^3)}{dt} = \langle \sigma v \rangle n_1^{\text{eq.}} n_2^{\text{eq.}} \left( \frac{n_3 n_4}{n_3^{\text{eq.}} n_4^{\text{eq.}}} - \frac{n_1 n_2}{n_1^{\text{eq.}} n_2^{\text{eq.}}} \right) \quad (5.1.1)$$

In this context, the cross section  $\sigma v$  is shared between the process  $\chi_1\chi_2 \rightarrow \chi_3\chi_4$  and its time-reversed counterpart  $\chi_3\chi_4 \rightarrow \chi_1\chi_2$ , assuming time reversal invariance. The number densities denoted with the superscript <sup>eq.</sup> correspond to those in thermal equilibrium.

In our scenario,  $\chi_{3,4}$  represent typical light (relativistic) particles in the thermal bath, making  $n_{3,4} = n_{3,4}^{\text{eq.}}$ . Additionally, we account for the annihilation process  $\chi\chi \leftrightarrow (\text{mundane})^2$ , leading to  $n_1 = n_2$ . Consequently, the Boltzmann equation is significantly simplified to

$$a^{-3} \frac{dn_\chi a^3}{dt} = \langle \sigma_{ann} v \rangle \left[ (n_\chi^{\text{eq.}})^2 - (n_\chi)^2 \right] \quad (5.1.2)$$

We use

$$Y = \frac{n_\chi}{s} \quad (5.1.3)$$

$$s = g_* T^3 \left( \frac{2\pi^2}{45} \right) \quad (5.1.4)$$

$$H^2 = \frac{8\pi}{3} G_N g_* \frac{\pi^2}{30} T^4 = g_* \frac{\pi^2}{90} \frac{T^4}{M_{Pl}^2} \quad (5.1.5)$$

$$x = \frac{m_\chi}{T} \quad (5.1.6)$$

Despite beginning at temperatures  $T > m_\chi$  when  $\chi$  particles are relativistic, as the temperature decreases below  $m_\chi$ , we transition to using non-relativistic approximations. At this point, the equilibrium number density can be straightforwardly determined as

$$n_\chi^{\text{eq.}} = \int \frac{d^3p}{(2\pi)^3} e^{-E/T} \left( E = m_\chi + \frac{\vec{p}^2}{2m_\chi} \right) \quad (5.1.7)$$

$$= e^{-m_\chi/T} \left( \frac{m_\chi T}{2\pi} \right)^{3/2} = e^{-x} \frac{m_\chi^3}{(2\pi x)^{3/2}} \quad (5.1.8)$$

Therefore

$$Y_{\text{eq.}} = \frac{n_\chi^{\text{eq.}}}{s} = \frac{1}{g_*} \frac{45}{2\pi^2} \left( \frac{x}{2\pi} \right)^{3/2} e^{-x} = 0.145x^{3/2}e^{-x} \quad (5.1.9)$$

By substituting the variables  $n_\chi$  with  $Y$  and  $t$  with  $x$ , the Boltzmann equation transforms as follows:

$$\frac{dY}{dx} = -\frac{1}{x^2} \frac{s(m_\chi)}{H(m_\chi)} \langle \sigma_{\text{ann}} v \rangle (Y^2 - Y_{\text{eq.}}^2) \quad (5.1.10)$$

Here,  $s(T) = s(m_\chi)/x^3$  and

$$dt = -\frac{1}{H(T)} \frac{dT}{T} = -\frac{m_\chi^2}{H(m_\chi) T^3} dT = \frac{1}{H(m_\chi)} x dx \quad (5.1.11)$$

It is useful to work out

$$\frac{s(m_\chi)}{H(m_\chi)} = \frac{2\pi^2}{45} \left( \frac{90}{\pi^2} \right)^{1/2} g_*^{1/2} m_\chi M_{Pl} = 1.32g_*^{1/2} m_\chi M_{Pl} \quad (5.1.12)$$

Note that the annihilation cross section  $\langle\sigma_{ann}v\rangle$  remains insensitive to temperature once the particle becomes non-relativistic ( $T \ll m_\chi$ ). Therefore, the entire combination  $\frac{s(m_\chi)}{H(m_\chi)} \langle\sigma_{ann}v\rangle$  is merely a dimensionless number. The main complication arises from the strong dependence of  $Y_{eq.}$  on  $x$ . To streamline the equation, we introduce the quantity

$$y = \frac{s(m_\chi)}{H(m_\chi)} \langle\sigma_{ann}v\rangle Y \quad (5.1.13)$$

We obtain

$$\frac{dy}{dx} = -\frac{1}{x^2} (y^2 - y_{eq.}^2) \quad (5.1.14)$$

with

$$y_{eq.} = 0.192g_*^{-1/2} M_{Pl} m_\chi \langle\sigma_{ann}v\rangle x^{3/2} e^{-x} \quad (5.1.15)$$

## 5.1.2 Numerical Integration

Next, we proceed with the numerical integration of the Boltzmann equation<sup>1</sup>. Figure 5.1 illustrates the evolution of  $y$  with respect to  $x$ . Initially, we observe that it closely follows the equilibrium value; however, after reaching an  $x$  value of approximately 20, significant deviations begin to appear, eventually stabilizing at a constant value. This behavior precisely mirrors the expected outcomes from our analytic approximations.

Putting everything back,

$$\rho_\chi = m_\chi n_\chi = m_\chi Y s = m_\chi \frac{H(m_\chi)}{s(m_\chi)} \frac{x_f}{\langle\sigma_{ann}v\rangle} s \quad (5.1.16)$$

---

<sup>1</sup>The numerical solution is in the mathematica file here: <https://shorturl.at/fGTY0>

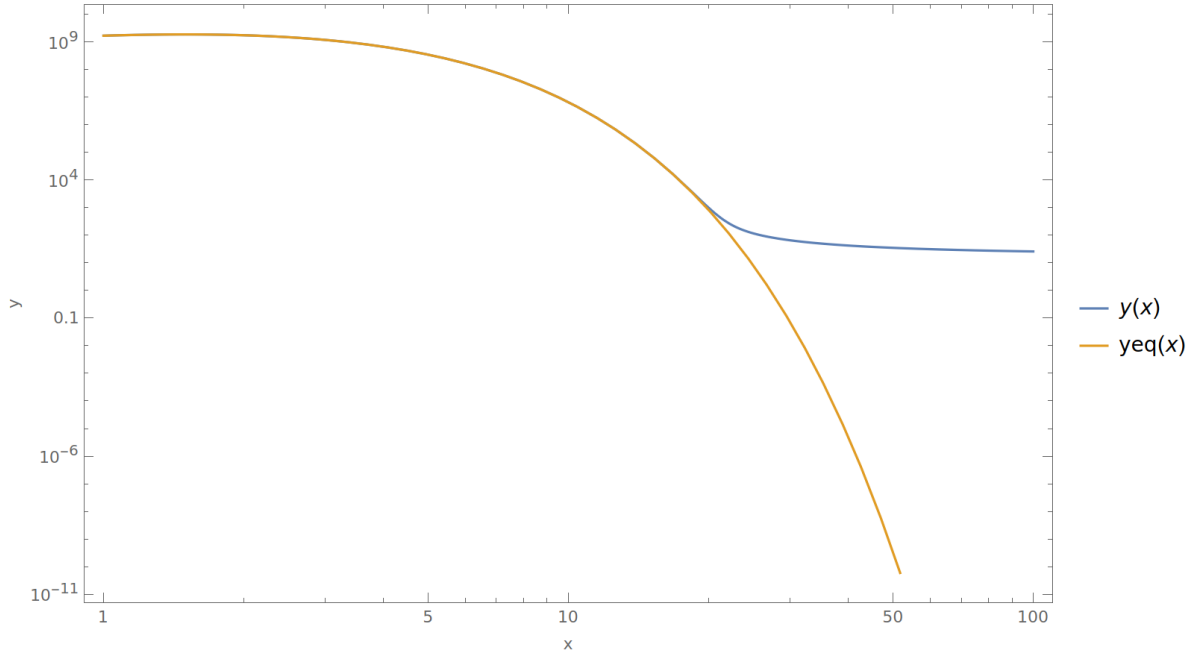


Figure 5.1: A numerical solution to the Boltzmann equation is applied for parameters where  $m = 100\text{GeV}$ ,  $g_* = 100$ , and  $\langle\sigma_{ann}v\rangle = 10^{-9}\text{GeV}^{-2}$ . Overlaid on this solution is the equilibrium value  $y_{\text{eq}}$ .

We use  $s_0 = 2890\text{ cm}^{-3}$  and  $\rho_c = 1.05 \times 10^{-5}h^2\text{GeVcm}^{-3}$ , where the current Hubble constant is  $H_0 = 100h\text{ km/sec/Mpc}$  with  $h \approx 0.65$ . To obtain  $\Omega_M h^2 \sim 0.12$  [11], we find  $\langle\sigma_{ann}v\rangle = 1.6 \times 10^{-9}\text{GeV}^{-2}$ .

This phenomenon is commonly known as the “WIMP miracle”: assuming a dark matter particle with a mass at the electroweak scale and an annihilation process mediated by the weak interaction, the predicted relic density matches the observed value precisely.

## 5.2 DM- $\nu$ decoupling

Now, our objective is to determine the temperature at which neutrinos decouple from dark matter (DM), utilizing the cross-section data from [14]. To achieve this, we will equate the interaction rate between neutrinos and

dark matter to the Hubble rate. Interaction and Hubble rates are given by

$$\Gamma = n\langle\sigma v\rangle \quad \text{and} \quad H = \sqrt{\frac{8\pi G}{3}\rho} \quad (5.2.1)$$

where  $\langle\sigma v\rangle$  is the thermally averaged annihilation cross section,  $n$  and  $\rho$  are the number and energy density of neutrino respectively.

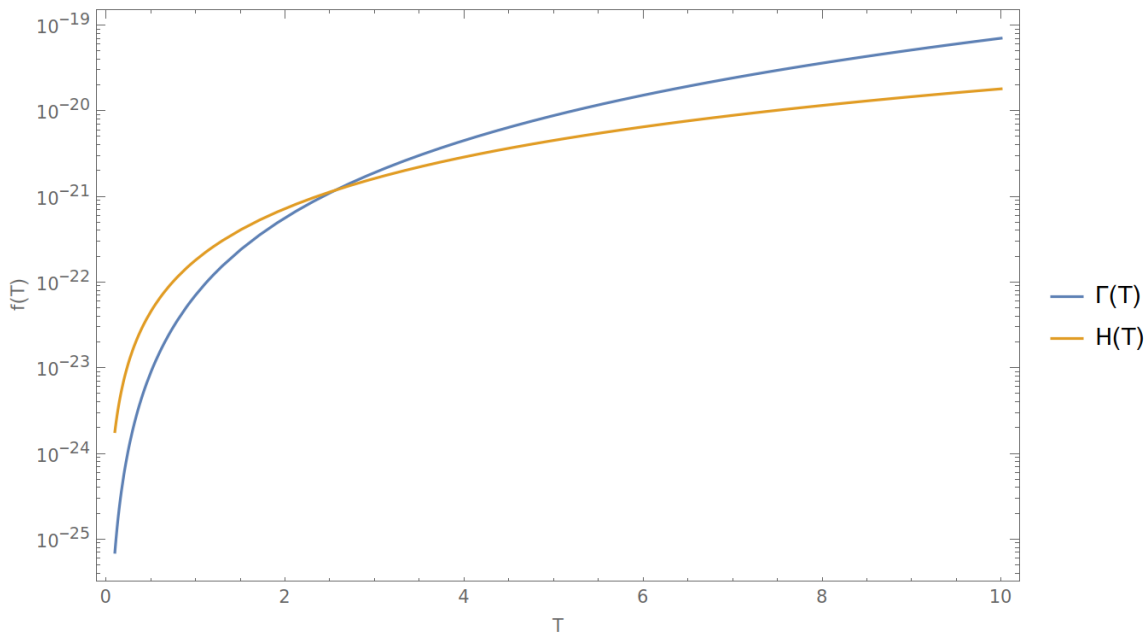


Figure 5.2: The decoupling of neutrino from DM

We observed that for DM mass of 0.5 MeV, neutrino decouples around  $\approx 2.5$  MeV and that means neutrino decouple from DM when it was still relativistic and considered as a hot relic.<sup>2</sup>

### 5.3 Effective number of neutrinos: $N_{\text{eff}}$

In standard cosmology, neutrinos undergo decoupling from the rest of the Standard Model (SM) particles at a temperature  $T_{\text{dec}} \approx 2.3$  MeV, with the effective number of neutrinos evaluated to be  $N_{\text{eff}} = 3.045$ . In scenarios involving thermal Dark Matter (DM) that remains in equilibrium with

---

<sup>2</sup>The calculation has been done in Mathematica which can be found here: <https://shorturl.at/uzGVW>

neutrinos even below  $T_{\text{dec}}$ , there is an entropy transfer from the dark sector to the neutrinos [13].

When considering only relativistic neutrinos and photons, with their distribution functions characterized by their respective temperatures, the effective number of neutrinos  $N_{\text{eff}}$  is expressed as:

$$N_{\text{eff}} = 3 \left( \frac{11}{4} \right)^{4/3} \left( \frac{T_\nu}{T_\gamma} \right)^4 \quad (5.3.1)$$

The Planck satellite has provided exceptionally precise measurements of  $N_{\text{eff}}$ . In the Planck 2018 analysis, different combinations of data sets were examined within the  $\Lambda$ CDM framework. For our investigation, we will utilize the Planck 2018  $N_{\text{eff}}$  constraints derived from the combination of TT+TE+EE+lowE+lensing+BAO: [5]

$$N_{\text{eff}} = 2.99_{-0.33}^{+0.34} \quad (95\% \text{CL, TT} + \text{TE} + \text{EE} + \text{lowE} + \text{lensing} + \text{BAO}) \quad (5.3.2)$$

Using the bounds on  $N_{\text{eff}}$ , we can set the bounds on current neutrino temperature:

$$T_\nu = 1.945 \text{K}_{-0.126}^{+0.207} \quad (5.3.3)$$

Considering neutrinos massless, their number density as a function of temperature is given by

$$n = \frac{3}{4\pi^2} \frac{g\zeta(3)}{\hbar^3 c^3} (k_B T_\nu)^3 \quad (5.3.4)$$

The standard number density of neutrinos is  $n_0 \approx 56 \text{cm}^{-3}$ . After plugging

in  $T_\nu = 1.945\text{K}_{-0.126}^{+0.207}$ , we get

$$n_+ \approx 70\text{cm}^{-3} \quad (5.3.5)$$

$$n_- \approx 46\text{cm}^{-3} \quad (5.3.6)$$

where  $n_+$  represent the enhancement case for number density with  $T_\nu = (1.945 + 0.207)\text{K}$  and  $n_-$  represent the suppression case for number density with  $T_\nu = (1.945 - 0.126)\text{K}$ .

## 5.4 Evidence of DM- $\nu$ interaction on PTOLEMY

If the interaction of a species freezes out (i.e.,  $\Gamma < H$ ) at a temperature where  $m/T \ll 1$ , then the species can exhibit a substantial relic abundance today. Now, we will compute the relic abundance for neutrinos in the scenario of their interaction with Dark Matter (DM) during the early universe.

Only annihilation and inverse annihilation processes, such as



can change the number of  $\nu$ 's and  $\bar{\nu}$ 's in a comoving volume. We will also assume that DM have thermal distributions with zero chemical potential. We have the Boltzmann eq. in Eq. 5.1.10

$$\frac{dY}{dx} = -\frac{1}{x^2} \frac{s(m_\chi)}{H(m_\chi)} \langle \sigma_{ann} v \rangle (Y^2 - Y_{\text{eq.}}^2) \quad (5.4.2)$$

In the highly relativistic regime ( $x \ll 1$ ), the equilibrium number density of neutrinos per comoving volume can be described by the following simplified

limiting form:

$$Y_{\text{eq.}}(x) = \frac{n_{\nu}^{\text{eq.}}}{s} \quad (5.4.3)$$

$$Y_{\text{eq.}}(x) = \frac{g_{\text{eff}}\zeta(3)}{\pi^2}T^3 / \frac{2\pi^2}{45}g_*T^3 \quad (5.4.4)$$

$$Y_{\text{eq.}}(x) = 0.278\frac{g_{\text{eff}}}{g_*} \quad (5.4.5)$$

where  $g_{\text{eff}} = g$  (bosons) and  $g_{\text{eff}} = 3g/4$  (fermions).

The Boltzmann equation governing the evolution of species abundance represents a specific form of the Riccati equation, lacking general closed-form solutions. The annihilation rate  $\Gamma$  is proportional to  $n^{\text{eq.}}$ , the equilibrium number density, multiplied by the thermally averaged annihilation cross section. In the relativistic regime,  $n^{\text{eq.}} \sim T^3$ , and in the non-relativistic regime,  $n^{\text{eq.}} \sim (mT)^{3/2} \exp(-m/T)$ , causing  $\Gamma$  to decrease exponentially with decreasing temperature  $T$ . Ultimately, as  $T$  decreases,  $\Gamma$  diminishes to a point where annihilations become negligible, approximately when  $\Gamma \approx H$  at  $x = x_f$  (referred to as “freeze-out”).

Consequently, we anticipate that for  $x \leq x_f$ , the abundance  $Y$  approaches  $Y_{\text{eq.}}$ , while for  $x \geq x_f$ , the abundance “freezes-in” to  $Y(x \geq x_f) = Y_{\text{eq.}}(x_f)$ . For neutrinos, when  $x_f \ll 1$ , freeze-out occurs while the neutrinos are still relativistic and the quantity  $Y_{\text{eq.}}$  remains constant. In such a scenario, the final value of  $Y$  is not strongly dependent on the specifics of the freeze-out process. The asymptotic value of  $Y$ , denoted as  $Y_0$ , simply corresponds to the equilibrium value at freeze-out,

$$Y_0 = Y_{\text{eq.}}(x_f) = 0.278\frac{g_{\text{eff}}}{g_*(x_f)} \quad (5.4.6)$$

where we take  $g=1$  (not considering anti-neutrino) and  $g_*(x_f) = 1 + 2 + 7/8(6 + 4)$  (where 1 is for scalar DM, 2 for photons, 6 for neutrinos and 4 for electron-positron pair) at the time of neutrino decoupling with DM.

Assuming the constant entropy per comoving volume, the abundance of

neutrino's today would be

$$n'_0 = s_0 Y_0 \approx 51 \text{cm}^{-3} \quad (5.4.7)$$

where  $n'_0$  represent the suppressed number density of neutrinos and  $s_0$  is the current entropy density,  $s_0 = 2890 \text{ cm}^{-3}$  [11].

Now we can calculate the capture rate of neutrinos in PTOLEMY in case of suppression of number density of neutrinos which is given by

$$\Gamma = \bar{\sigma} n'_0 N_T c \quad (5.4.8)$$

where  $\bar{\sigma} = \sigma v = 3.834 \times 10^{-45} \text{cm}^2$  is the neutrino capture cross-section on tritium,  $N_T$  is the total number of tritium nuclei and  $c$  is the speed of light  
For 100gm of tritium

$$N_T = \frac{100}{3 \times 1.66 \times 10^{-24}} = 2 \times 10^{25} \quad (5.4.9)$$

The suppressed capture rate would be

$$\Gamma_{C\nu B}^{D'} \approx 3.70 \text{ yr}^{-1} \quad \text{and} \quad \Gamma_{C\nu B}^{M'} \approx 7.40 \text{ yr}^{-1} \quad (5.4.10)$$

where  $\Gamma_{C\nu B}^{D'}$  and  $\Gamma_{C\nu B}^{M'}$  are the suppressed capture rate for Dirac and Majorana neutrino cases, respectively.

# Chapter 6

## Results and Discussion

The interactions between dark matter (DM) and neutrinos, particularly around the time of neutrino decoupling from the Standard Model (SM), play a significant role in altering the effective number of neutrino species ( $N_{\text{eff}}$ ) by exchanging entropy with the neutrino bath. Our investigation reveals that these interactions have implications for understanding the evolution of neutrino properties and their impact on experimental observations.

The constraints on  $N_{\text{eff}}$  derived from the Planck 2018 data have significant implications for our understanding of neutrino properties and cosmological models. By considering the bounds on  $N_{\text{eff}}$ , we can explore how variations in the effective number of neutrino species impact the temperature of the neutrino background. This investigation reveals the potential for altering the neutrino number density, which is typically estimated at around 70 neutrinos per cubic centimeter under enhanced conditions and 46 neutrinos per cubic centimeter under suppressed conditions. This range is exploitable from the perspective of DM- $\nu$  interactions.

Our analysis suggest that the interaction between a scalar dark matter (which remains relativistic around Neutrino decoupling) and neutrinos during the early universe results in a notable 9% alteration in the current number density of neutrinos. Further it implies that these interactions

could lead to a reduction in the capture rate of neutrinos. Specifically, after 10 years of operation, PTOLEMY could potentially observe 3 fewer events in the case of Dirac neutrinos and 7 fewer events in the case of Majorana neutrinos due to these interactions.

A reduction in the capture rate of neutrinos at PTOLEMY would provide a tangible observation reflecting the impact of scalar DM-neutrino interactions on neutrino behavior. This result highlights the potential influence of dark matter on neutrino properties and underscores the importance of further investigating such interactions to deepen our understanding of fundamental particle dynamics in the cosmos.

These findings suggest intriguing observations, and we intend to submit them for publication in a research journal in the future.

# Appendix A

## Cross section for neutrino capture on tritium

In the neutrino capture experiment under consideration, the spins of the final state electron and nucleus are not observed or measured. Consequently, it becomes necessary to sum over all potential final states. Likewise, since the initial nucleus is not initially prepared with a definite spin, we must also sum over its two potential spin states.

Unlike Dirac neutrinos, which are prepared in a definite spin state (specifically left-helical), Majorana neutrinos exhibit both helicities. We will maintain a general approach to the calculation for now. The neutrino helicity, denoted by  $s_\nu$ , takes values where  $s_\nu = +1/2$  corresponds to right-handed helicity and  $s_\nu = -1/2$  corresponds to left-handed helicity.

$$|M|^2 = \frac{G_F^2}{2} |V_{ud}|^2 |U_{ej}^*|^2 T_1^{\alpha\gamma} T_2^{\beta\delta} \eta_{\alpha\beta} \eta_{\gamma\delta} \quad (\text{A.0.1})$$

where

$$T_1^{\alpha\gamma} = Tr[\gamma^\alpha (1 - \gamma^5) u_\nu \bar{u}_\nu \gamma^\gamma (1 - \gamma^5) u_e \bar{u}_e] \quad (\text{A.0.2})$$

$$T_2^{\beta\delta} = Tr[\gamma^\beta (f - g\gamma^5) u_n \bar{u}_n \gamma^\delta (f - g\gamma^5) u_p \bar{u}_p] \quad (\text{A.0.3})$$

To simplify the presentation, we have omitted the index  $j$  that specifies the neutrino mass eigenstate.

$$|\overline{M}|^2 = \frac{1}{2} \sum_{s_n, s_e, s_p = \pm 1/2} |M|^2 = \frac{G_F^2}{4} |V_{ud}|^2 |U_{ej}^*|^2 \overline{T_1^{\alpha\gamma}} \overline{T_2^{\beta\delta}} \eta_{\alpha\beta} \eta_{\gamma\delta} \quad (\text{A.0.4})$$

where

$$\overline{T_1^{\alpha\gamma}} = \sum_{s_e = \pm 1/2} \text{Tr}[\gamma^\alpha (1 - \gamma^5) u_\nu \bar{u}_\nu \gamma^\gamma (1 - \gamma^5) u_e \bar{u}_e] \quad (\text{A.0.5})$$

$$\overline{T_2^{\beta\delta}} = \sum_{s_n, s_p = \pm 1/2} \text{Tr}[\gamma^\beta (f - g\gamma^5) u_n \bar{u}_n \gamma^\delta (f - g\gamma^5) u_p \bar{u}_p] \quad (\text{A.0.6})$$

We now need to use the completeness relations.

$$\sum_{s_i = \pm 1/2} u_i \bar{u}_i = (p_i + M_i) \quad (\text{A.0.7})$$

for  $i=n,p,e$

$$u_\nu \bar{u}_\nu = 1/2(p_\nu + M_\nu)(1 + 2s_\nu \gamma^5 S_\nu) \quad (\text{A.0.8})$$

where

$$(S_\nu)^\alpha = \left( \frac{|p_\nu|}{m_\nu}, \frac{E_\nu}{m_\nu} \hat{p}_\nu \right) \quad (\text{A.0.9})$$

is the neutrino spin vector. Inserting these yields

$$\overline{T_1^{\alpha\gamma}} = \frac{1}{2} \text{Tr}[\gamma^\alpha(1 - \gamma^5)(p_\nu + m_\nu)(1 + 2s_\nu\gamma^5 S_\nu)\gamma^\gamma(1 - \gamma^5)(p_e + m_e)] \quad (\text{A.0.10})$$

$$\overline{T_2^{\beta\delta}} = \text{Tr}[\gamma^\beta(f - g\gamma^5)(p_n + m_n)\gamma^\delta(f - g\gamma^5)(p_p + m_p)] \quad (\text{A.0.11})$$

The evaluations of the traces are performed using the Mathematica package "FeynCalc," leading to the following results:<sup>1</sup>

$$\overline{T_1^{\alpha\gamma}}\overline{T_2^{\beta\delta}}\eta_{\alpha\beta}\eta_{\gamma\delta} = 32((f + g)^2(p_e \cdot p_p)(p_n \cdot p_\nu - 2m_\nu s_\nu(p_n \cdot S_\nu)) \quad (\text{A.0.12})$$

$$+ (f - g)((f - g)(p_e \cdot p_n)(p_p \cdot p_\nu - 2m_\nu s_\nu(p_p \cdot S_\nu)) \quad (\text{A.0.13})$$

$$- (f + g)m_n m_p(p_e \cdot p_\nu - 2m_\nu s_\nu(p_e \cdot S_\nu))) \quad (\text{A.0.14})$$

$$\begin{aligned} \overline{T_1^{\alpha\gamma}}\overline{T_2^{\beta\delta}}\eta_{\alpha\beta}\eta_{\gamma\delta} = 32 & [(f + g)^2[(p_e \cdot p_p)(p_\nu \cdot p_n)] + (g - f)^2[(p_e \cdot p_n)(p_\nu \cdot p_p)] \\ & + (g^2 - f^2)[m_n m_p(p_e \cdot p_\nu)] - 2s_\nu m_\nu [(g + f)^2[(p_e \cdot p_p)(S_\nu \cdot p_n)] \\ & + (g - f)^2[(p_e \cdot p_n)(S_\nu \cdot p_p)] + (g^2 - f^2)[m_n m_p(p_e \cdot S_\nu)]]] \end{aligned} \quad (\text{A.0.15})$$

We proceed by defining the rest frame of the neutron

$$(p_n)^\mu = (m_n, 0), \quad (p_\nu)^\mu = (E_\nu, p_\nu), \quad (p_p)^\mu = (E_p, p_p), \quad (p_e)^\mu = (E_e, p_e)$$

Ignoring the proton recoil ( $p_p \gg m_p$ ), we derive

---

<sup>1</sup>This is the mathematica file for the evaluation of traces: <https://shorturl.at/lvBO8>

$$\begin{aligned}
 \overline{|M|^2} = & 8G_F^2 |V_{ud}|^2 |U_{ej}^*|^2 m_n m_p E_e E_\nu \left( 2(g^2 + f^2) + (g^2 - f^2) \left[ 1 - \frac{p_e \cdot p_\nu}{E_e E_\nu} \right] \right) \\
 & - 2s_\nu m_n m_p E_e |p_\nu| \left( 2(g^2 + f^2) + (g^2 - f^2) \left[ 1 - \frac{E_\nu}{|p_\nu|} \frac{p_e \cdot p_\nu}{E_e |p_\nu|} \right] \right)
 \end{aligned} \tag{A.0.16}$$

Defining  $\cos\theta = \frac{p_e \cdot p_\nu}{|p_e| |p_\nu|}$  and  $v_i = \frac{|p_i|}{E_i}$ , we get

$$\begin{aligned}
 \overline{|M|^2} = & 8G_F^2 |V_{ud}|^2 |U_{ej}|^2 m_n m_p E_e E_\nu \left[ (f^2 + 3g^2)(1 - 2s_\nu v_\nu) \right. \\
 & \left. + (f^2 - g^2)(v_\nu - 2s_\nu)v_e \cos\theta \right]
 \end{aligned} \tag{A.0.17}$$

In this context,  $\theta$  represents the angle between the momenta of the neutrino and electron, while  $v_i$  denotes the velocity of the species  $i$ .

Now we can write

$$\begin{aligned}
 \overline{|M_j|^2}(s_\nu) = & 8G_F^2 |V_{ud}|^2 |U_{ej}|^2 m_n m_p E_e E_\nu \left[ A(s_\nu)(f^2 + 3g^2) + B(s_\nu)(f^2 - g^2)v_e \right. \\
 & \left. \cos\theta \right]
 \end{aligned} \tag{A.0.18}$$

# Bibliography

- [1] Kensuke Akita, Saul Hurwitz, and Masahide Yamaguchi. Precise Capture Rates of Cosmic Neutrinos and Their Implications on Cosmology. *Eur. Phys. J. C*, 81(4):344, 2021.
- [2] E. Baracchini et al. PTOLEMY: A Proposal for Thermal Relic Detection of Massive Neutrinos and Directional Detection of MeV Dark Matter. 8 2018.
- [3] Bruce A. Bassett and Renée Hlozek. Baryon acoustic oscillations, 2009.
- [4] M. G. Betti et al. Neutrino physics with the PTOLEMY project: active neutrino properties and the light sterile case. *JCAP*, 07:047, 2019.
- [5] Céline Boehm, Matthew J. Dolan, and Christopher McCabe. A Lower Bound on the Mass of Cold Thermal Dark Matter from Planck. *JCAP*, 08:041, 2013.
- [6] Scott Burles, Kenneth M. Nollett, and Michael S. Turner. Big-bang nucleosynthesis: Linking inner space and outer space, 1999.
- [7] Daniel J. Eisenstein and Zehavi... Detection of the baryon acoustic peak in the large-scale correlation function of sdss luminous red galaxies. *The Astrophysical Journal*, 633(2):560–574, November 2005.
- [8] R. Lazauskas, P. Vogel, and C. Volpe. Charged current cross section

- for massive cosmological neutrinos impinging on radioactive nuclei. *J. Phys. G*, 35:025001, 2008.
- [9] Mariangela Lisanti. Lectures on Dark Matter Physics. In *Theoretical Advanced Study Institute in Elementary Particle Physics: New Frontiers in Fields and Strings*, pages 399–446, 2017.
- [10] Andrew J. Long, Cecilia Lunardini, and Eray Sabancilar. Detecting non-relativistic cosmic neutrinos by capture on tritium: phenomenology and physics potential. *JCAP*, 08:038, 2014.
- [11] Hitoshi Murayama. Physics Beyond the Standard Model and Dark Matter. In *Les Houches Summer School - Session 86: Particle Physics and Cosmology: The Fabric of Spacetime*, 4 2007.
- [12] Andrés Olivares-Del Campo, Céline Boehm, Sergio Palomares-Ruiz, and Silvia Pascoli. Dark matter-neutrino interactions through the lens of their cosmological implications. *Phys. Rev. D*, 97(7):075039, 2018.
- [13] Sujata Pandey, Siddhartha Karmakar, and Subhendu Rakshit. Interactions of astrophysical neutrinos with dark matter: a model building perspective. *JHEP*, 01:095, 2019. [Erratum: *JHEP* 11, 215 (2021)].
- [14] Arnab Paul, Arindam Chatterjee, Anish Ghoshal, and Supratik Pal. Shedding light on dark matter and neutrino interactions from cosmology. *Journal of Cosmology and Astroparticle Physics*, 2021(10):017, October 2021.
- [15] R. Schiavilla, V. G. J. Stoks, W. Glöckle, H. Kamada, A. Nogga, J. Carlson, R. Machleidt, V. R. Pandharipande, R. B. Wiringa, A. Kievsky, S. Rosati, and M. Viviani. Weak capture of protons by protons. *Physical Review C*, 58(2):1263–1277, August 1998.